

# A Health-Aware Control Strategy for Enhanced Performance and Extended Hybrid Powertrain Lifecycle

A benchmark of different cost functions

A.M. Postma





Thesis for the degree of MSc in Marine Technology in the specialization of *Marine Engineering*

# A Health-Aware Control Strategy for Enhanced Performance and Extended Hybrid Powertrain Lifecycle

by

A.M. Postma

Performed at

## Delft University of Technology

This thesis (MT.22/23.041.M.) is classified as confidential in accordance with the general conditions for projects performed by the TUDelft.

Thursday 27<sup>th</sup> July, 2023

### Daily supervisor

Responsible supervisor: Dr. ir. A. Coraddu I

### Thesis exam committee:

Chair/Responsible professor Dr. ir. A. Coraddu

Staff Member: Dr. ir. L. van Biert

External member: Prof. L. Oneto (University of Genoa)

### Author Details

Studynumber 4570146

An electronic version of this thesis is available at <http://repository.tudelft.nl/>.

Front page image recovered from  
<https://www.sailinginnovationcentre.nl/h2c-boat/prototype/>



# Preface

Climate change is an ongoing topic for us all. More and more, people are beginning to find a way to contribute to the prevention of the effects of our behaviour on the world around us. However, the problem is more complex than most people (me included) think, as uncertainty around developments, but also the uncertainty around secondary or tertiary impacts (such as material usage, or installment) are getting more and more attention. Consider, for example, the effects of deep-sea mining, versus the necessity of cobalt for the development of electrical storage and generating devices.

It is therefore more important than ever to be able to predict the impact of certain measures, ideas, or solutions. What kind of impact and how to predict that impact is still, to this day, a question to be answered. This need for objective impact measurements initiates the need for independent research of which the only goal is to ensure a better future for our world. Solving a global crisis should not and never be about patents or earning millions. I am therefore proud to present a thesis in which the secondary and tertiary effects are considered, which is available for everyone who would like to use the findings.

I want to thank my supervisor Andrea Coraddu for his guidance. I want to thank my friends for the several years (and counting) of support and a special thanks to my girlfriend for dealing with my grumpy stress.

Finally, a huge thank you to my family, because as of today I am officially an **engineer**.

*A.M. Postma  
Delft, July 2023*



# Summary

To answer the 2050 goals set by the International Maritime Organization (IMO), power plant architectures are becoming more and more complex. These complex architectures also generate an increase in possible control strategies, and a proper design of these control systems can deliver significant fuel savings. One of the novelties in literature is to make the control systems aware of the health status of the power plant. This can result in two advantages: a longer lifetime of the components and fuel savings due to better loading of the same components. This health awareness can be accomplished using either a prognostic or a diagnostic approach. Literature seems to prefer the prognostic methods and therefore diagnostic methods are missing. This thesis aims to show that diagnostic methods do have a future when it comes to being applied in energy management systems (EMSs), which are the control systems of complex architectures.

To show the effects of the diagnostic system, a test case power plant which is based on the H2C boat and consists of a 20 kW fuel cell and a 40 kWh battery is used to benchmark a not health aware, new health aware, and a health aware energy management system from literature. To accurately develop a digital twin of this boat, different methods, both for degradation and efficiency have been researched. For the efficiency models, there are quite some accurate models that manage to accomplish results that are close to the data in accuracy, but the models are not able to capture real-life degradation yet. However, these models are, although slightly altered, still used to describe the degradation of the components, as there are no better models available yet.

The actual EMS developed in this thesis focuses on two aspects: aim to minimize actual known degradation mechanisms instead of models, and secondly aim to have a constant weight for each objective over the power plant lifetime, as each objective should always be equally important. It does so by stating three objectives: maximize fuel cell efficiency, minimize fuel cell power fluctuations, and penalize a high state of charge. By stating a multi-objective EMS and assigning different weights to this multi-objective EMS, a paretofront can be created. The best result of this paretofront can be chosen based on different costs for the objectives, which are allowed and should be altered in future work. An important note here is that, for future research, these costs (and thus the weights) should not be fixed, as accurate predictions about the price of different components are hard to make. The best result can eventually be compared to the EMS from literature and the EMS that does not take health into account.

The results show that the developed EMS manages to outperform the not health-aware EMS on different key performance indices (KPIs), but only manages to outperform the EMS from literature on a few of these KPIs. This also shows the problem with the current health-aware EMS research. As little is known about fuel cell and battery degradation, it becomes difficult to quantitatively measure the performance of an EMS. Most research solves this by measuring the performance of KPIs that are defined by the research, thus resulting in subjective results.

Consequently, this research concludes that further investigation is necessary for component degradation. This would enable improved models capable of estimating the current component health based on various parameters. Additionally, it would empower EMSs to better comprehend the impact of their operations by penalizing specific operating conditions that are known to have a substantial negative effect on the lifespan of the power plant.

In summary, this research contributes to the understanding of the impact of health-aware energy management systems. Instead of the popular prognostic approach, this thesis aimed at using a diagnostic approach whilst also suggesting known and new mathematical models for powerplant components in a fuel cell and battery hybrid ship. Conclusively, it suggests avenues for future investigation. By following these avenues, the development of more effective and unbiased health-aware EMSs can be realized.



# Contents

<b>Preface</b>	<b>iii</b>
<b>Summary</b>	<b>v</b>
<b>1 Introduction</b>	<b>1</b>
<b>2 Health aware energy management systems</b>	<b>3</b>
2.1 General energy management systems . . . . .	3
2.2 Rule based strategies . . . . .	4
2.3 Optimization-based strategies . . . . .	4
2.4 Machine Learning-based strategies . . . . .	5
2.5 Health aware EMS . . . . .	5
2.6 Conclusion . . . . .	6
<b>3 Methodology</b>	<b>7</b>
3.1 The ship . . . . .	7
3.2 The health-awareness problem . . . . .	8
3.3 Battery . . . . .	9
3.4 Fuel cell . . . . .	12
3.5 Conclusion . . . . .	16
<b>4 The EMS Functions</b>	<b>17</b>
4.1 Battery model . . . . .	17
4.2 Fuel cell model . . . . .	21
4.3 Not health-aware EMS . . . . .	24
4.4 Health-aware EMS . . . . .	25
4.5 EMS control strategy . . . . .	29
4.6 Conclusion . . . . .	30
<b>5 Results</b>	<b>31</b>
5.1 Grid convergence study. . . . .	31
5.2 Verification of the model . . . . .	32
5.3 Multi-objective optimization results. . . . .	35
5.4 Comparison between 3 EMS . . . . .	38
5.5 Conclusion . . . . .	41
<b>6 Discussion</b>	<b>43</b>
<b>7 Conclusion</b>	<b>47</b>
<b>Bibliography</b>	<b>48</b>
<b>A Pareto-fronts</b>	<b>59</b>
<b>B Health aware Energy Management Systems literature</b>	<b>61</b>



# List of Figures

2.1	Different energy management methods according to: Mustafa et al. [1]	3
2.2	Distribution of prognostic and diagnostic health aware EMS	6
3.1	Validation of the degradation function with and without data	8
3.2	General idea behind the energy management system	9
3.3	Rint model as found in Planakis et al. [2]	10
3.4	Ideal and Actual Fuel Cell Voltage according to Appleby and Foulkes [3]	13
4.1	Charging and discharging behaviour of a battery, data retrieved from McIntosh [4]	18
4.2	Comparison of the behaviour of the $SOC$ , $I_{bat}$ and $U_{OCV}$	18
4.3	Validation of the degradation function with and without data	20
4.4	Comparison of the power current, power hydrogen consumption and voltage-current relation of the fuel cell	22
4.5	Efficiency of different systems according to Appleby and Foulkes [3]	23
4.6	Comparison of the power current, power hydrogen consumption and voltage-current relation of the fuel cell with a BOP	23
5.1	Grid convergence study of the battery degradation, fuel cell degradation and hydrogen consumption using the not-health aware function	32
5.2	Results the first test case: maximize fuel consumption	33
5.3	Results of test case 2: maximize the power changes on the fuel cell	33
5.4	Results of test case 3: minimize hydrogen consumption	34
5.5	Results of test case 4: Run the optimization with and without degradation.	34
5.6	Generated Pareto front	35
5.7	Results of the hydrogen consumption per hour coming from the Postma health aware EMS	35
5.8	Differences in optimal power distribution between for the first optimization step of different $\lambda_2$ 's	36
5.9	Results of the fuel cell degradation per hour resulting from the Postma health aware EMS	36
5.10	Results of the battery degradation per hour resulting from the Postma health aware EMS	37
5.11	Cost of hydrogen according to Ajanovic et al. [5]	37
5.12	Hourly operating costs of the entire system using the Postma health aware function	38
5.13	Comparison of the resulting battery degradation, fuel cell degradation and hydrogen consumption of each EMS	39
5.14	Comparison of the power distributions of the different EMS	40
5.15	Resulting $SOC$ distribution of each EMS	41
6.1	Effects of changing the value of $M$	44
6.2	Relation between temperature and battery degradation according to Wang et al. [6]	44
A.1	Three different perspectives of the Pareto-front	59
B.1	Health aware EMS's	62



# List of Tables

3.1	EMS Battery models as found in literature . . . . .	10
3.2	Generalized life models for certain c-rates as found in Wang et al. [6] . . . . .	12
3.3	Most common degradation causes for fuel cells according to literature . . . . .	15
3.4	Degradation rates PEMFC . . . . .	16
4.1	Applied degradation rates for the fuel cell system . . . . .	24
4.2	Causes SEI layer formation according to literature . . . . .	28
4.3	Time response of different subsystems in a ship according to Bagherabadi et al. [7] . . . . .	30
5.1	Costs per day. . . . .	41



# Nomenclature

## Abbreviations

BOP	Balance Of Plant
BOP	Balance Of Plant
DOD	Depth Of Discharge
Crate	Discharge Rate
DP	Dynamic Programming
EMS	Energy Managent System
ECM	Equivalent Circuit Model
HEV	Hybrid Electric Vehicle
KPI	Key Performance Indicator
PEMFC	Proton Exchange Membrane Fuel Cell
RUL	Remaining Usefull Life
SEI	Solid Electrolyte Interphase
SOC	State Of Charge
SOH	State Of Health
ESS	Electronic storage solution
GHG	Green House Gasses
RB	Rule Based strategies
OB	Optimization Based strategies
MLB	Machine Learning Based
$N_x$	Number of grid points

## Physical constants

$F$	Farradays Constant	96,485	$C/mol$
$R$	Gas Constant	8.314	$J/(mol * K)$

## Variables

$Ah$	Ampère-Hours	$Ah$
$ASR$	Area Specific Resistance	$\Omega$
$C_n$	Battery Capacity	$Ah$
$I_{bat}$	Battery Current	$A$
$\eta_{bat}$	Battery Efficiency	-
$P_{bat}$	Battery Power	$W$
$T_{bat}$	Battery Temperature	$^{\circ}K$
$I_{FC}$	Fuel Cell Current	$A$
$V_{0FC}$	Fuel Cell Open Circuit Voltage	$V$
$R_{int}$	Internal Battery Resistance	$\Omega$
$V_{OCV}$	Open Battery Voltage	$V$
$B$	Pre-Exponential Factor	-
$Q_r$	Reaction quotient	-
$V_{OCV}$	Open Battery Voltage	$V$



# 1

## Introduction

According to the International Maritime Organization (IMO), in 2018 the global CO<sub>2</sub> emissions of shipping alone were equal to 1,056 million tonnes. This represented 2.89% of the total global CO<sub>2</sub> emissions. As the emissions caused by ships are expected to be 90 - 130% of their 2008 greenhouse emissions in 2050, the IMO aims to reduce this number to at least 50%. Different low greenhouse gas emitting energy generating systems are being investigated and developed to reach this number. Additionally, according to Geertsma et al. [9]: *'The operating profile of ships has become increasingly diverse [...] This trade-off between efficiency and adaptability to diverse operating profiles has led to a growing variety of power and propulsion architectures'*. This increase in the variety of power and propulsion architectures also leads to an increase in possible control strategies. Proper design and control systems for these architectures can deliver significant fuel savings to make ships greener and safer [10]. However, most architectures still use classical control theories, which according to Nguyen et al. [11] have many weaknesses such as not achieving the goals such as lower hydrogen consumption.

The architectures mentioned in the previous paragraph are described as hybrid power plants or hybrid ships. According to Inal et al. [12]: *'The integration of Energy Storage Systems (ESS) is a key point for hybrid ships'*. Later, the same author states: *'From the storage point of view, lead-acid batteries have not been considered for large-scale present and future applications due to limited power and energy density capacity. Indeed, Li-Ion batteries are a reference solution for hybrid ship ESS'*. The production of these Li-Ion batteries, however, has a large contribution to global greenhouse gases (GHG). For example, Peters et al. [13] have reviewed 79 papers on the environmental impact of the production of Li-Ion batteries, concluding that: *'The average cumulative energy demand (CED) and GHG emissions for battery production are 328 kWh and 110 kg CO<sub>2</sub> equivalent per kWh of storage capacity, respectively'*. Besides that, both the environmental and social impact on the areas where lithium is mined is not even discussed. As the goal is to solve the global crisis problems and not reallocate them, the lifetime of these batteries should be considered in the control system of the hybrid power plant.

Besides using ESS, the second focus in hybrid propulsion layouts of ships is using alternative fuels. One of those alternative fuels is hydrogen, which is used via fuel cells [14]. Kandidayeni et al. [15] states that: *'Ignorance of health adaptation can increase the hydrogen consumption from almost 6.5% to 24% depending on the Energy Management System (EMS)'*. And, as can be found in Wang et al. [16] the failure of one cell in a fuel cell stack, can lead to the replacement of the entire fuel cell stack, instead of the replacement of that component. Thus, again, the health of the components is an essential factor in the overall performance of the system.

As mentioned above, it is important to account for the health of components, or mitigate degradation, as this can prolong the lifespan and increase efficiency. Furthermore, one of the demotivating factors in the transition to hybrid propulsion is currently the limited lifetime Inal et al. [12]. And as stated by Kandidayeni et al. [15]: *'... the integration of health awareness factors into the EMS design has still a long way to go'*.

This thesis looks into the integration of component health into ship EMS design by answering the following research question:

*'What is the impact of including component degradation in advanced energy management strategies on energy consumption and power plant lifetime for fuel cell-battery powered vessels?'*

To answer this question, the following sub-questions form the basis for this thesis:

1. What is state-of-the-art in health aware energy management systems?
2. What method will be used to describe the powerplant and energy management system?
3. What are the mathematical models of the method that describe powerplants?

Through this approach, the thesis aims to comprehensively address the case modelling, EMS design, mathematical formulation, and optimization aspects, ultimately contributing two novelties to the reviewed literature:

- Introduction of a new derivative function for battery degradation.
- Instead of minimizing degradation models, the EMS developed in this thesis aims to penalize different causes of component degradation.

Chapter 2 introduces the state-of-the-art when it comes to health-aware EMSs, therefore answering sub-question 1. Chapter 3 will introduce the methodology that will be used for building the virtual power plant, thus answering sub-question 2. Chapter 4 will delve into the mathematical formulations underpinning the cost functions utilized in the optimization process and therefore answer sub-question 3. The mathematical foundations presented in this chapter will serve as a basis for the subsequent optimization analysis. Building upon the mathematical foundations laid out in Chapter 4, Chapter 5 will present the outcomes and findings of the final optimization process. This chapter will show the results obtained through the application of the developed EMS and optimization techniques. Additionally, these results will be evaluated using various key performance indicators (KPIs).

# 2

## Health aware energy management systems

This chapter introduces health aware EMSs by explaining the different EMS found in literature and how these systems account for the "health awareness" aspect. The final goal of this chapter is to find the literature gap and form the basis of the EMS that is introduced later in this thesis.

### 2.1. General energy management systems

EMS are responsible for the distribution of required power amongst the power-generating components in a power plant based on information analysis [15, 17, 18]. This can be applied to any sort of power plant and gets increasingly effective, but also complex, for hybrid power plants with more degrees of freedom [9]. The aim of the energy management system for this research comes in threefold:

1. Make sure that the ship can complete its mission;
2. Minimize energy consumption;
3. Minimize component degradation.

The EMSs can be divided into three different categories: Rule-based (RB), Optimization-based (OB) and Machine Learning-based (MLB) systems [1, 19]. These systems can be found in Figure 2.1. This chapter gives an overview of these three methods and their (dis-) advantages.

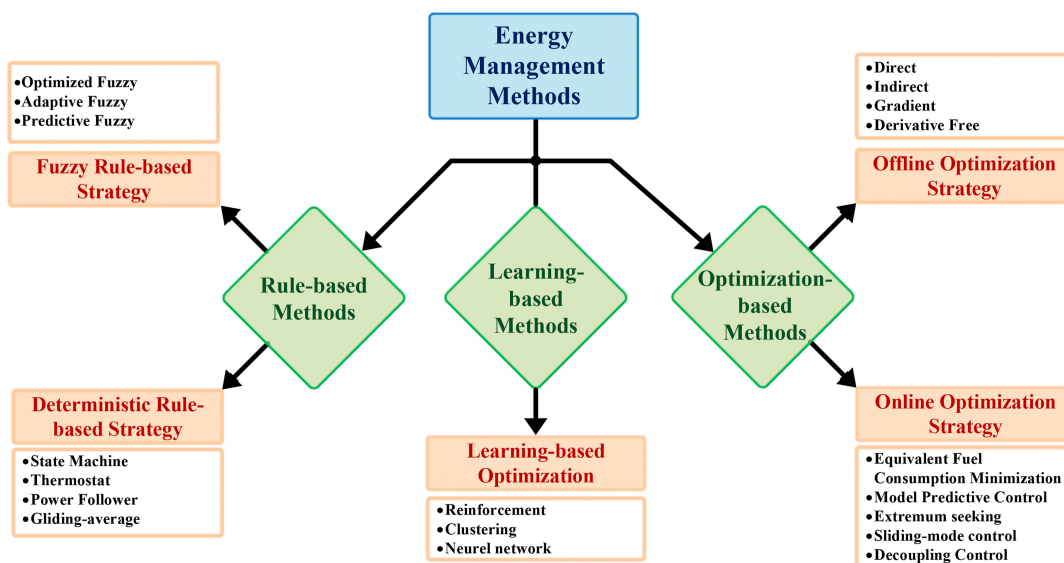


Figure 2.1: Different energy management methods according to: Mustafa et al. [1]

## 2.2. Rule based strategies

*RB control systems are robust and have a strong real-time performance* [12]. However, they also have disadvantages: according to [20] the effects of the rules are typically far away from the optimal control objectives. Or the systems have weak dynamic responses to changes [12] And finally, there is a necessity for a lot of expert knowledge in the design of the systems [21].

The RB control systems can be divided into two different strategies:

1. *Fuzzy rule based strategies: 'A method of judgement and reasoning by imitating the uncertainty in the human brain'* [21]. This entails that the fuzzy rules try to translate a non-binary statement into a statement that a binary system can understand. It creates a black box model based on 'human logic'. This model can also be trained by optimizing the rules for different drive cycles, thus ruling out the necessity for high expertise in the design phase. Yang et al. [22] uses the fuzzy rule strategy because of its high robustness and anti-disturbance capability. This resulted in slightly better energy efficiency than the conventional RB strategy.
2. *Deterministic Rule-based strategies* are strategies where the strategy follows a table or flow chart to determine which component will deliver what amount of power [21]. This strategy can be subdivided into the following:
  - (a) *Thermostat control: On/ off method.* Components turn on or off based on the state of the propulsion plant. Xie et al. [23] introduce a two-layer approach to EMS where the outer layer is a thermostat control layer in which the diesel-generator is turned on or off based on a set of rules that take the state of charge (SOC) of the battery and the load of the diesel engine into account. Although this method works for the automotive industry, it is less feasible for the diesel engines on a ship due to the high amount of energy needed to start up the engines (not even mentioning the amount of CO<sub>2</sub> produced when the engine is choking due to turbo-lag);
  - (b) *Power follower method:* Trovão and Pereirinha [24] applies the power follower method in an EMS for an HEV. This method considers for each situation the highest efficiency from a beforehand generated efficiency map.
  - (c) *Gliding average:* This method is also known as a moving average. When this method is applied, the load change on the components is minimized by taking the moving average of the requested load. Tritschler et al. [25] uses this method to smooth the load on a fuel cell, he concludes that the efficiency of the system is the same as for a general deterministic rule-based approach, with the limitation that the response of the fuel cell is delayed by the gliding average method.

The current trend in the rule-based literature is that the optimization of the rules is becoming less dependent on human expertise and more on machine learning algorithms. *"Due to the vast and rapid increase in data size, machine learning approaches have, thus, become increasingly popular towards the design of rule-based systems."* Liu et al. [26]

## 2.3. Optimization-based strategies

OB strategies optimize a cost function, that can be single or multi-objective. As reported in Figure 2.1 the OB strategies can be divided into two different categories: offline and online methods:

1. *Offline methods:* offline methods are often referred to as global OB strategies. They are designed to find the global optimal solution to the control problem for a known drive cycle. Because this algorithm requires future road and vehicle speed information, it can not be applied directly [27], but are still used to benchmark different EMS solutions. One of these solutions is dynamic programming, which is often used as a benchmark for other EMS's [17, 28, 29, 30]. It is also possible to use convex solvers for the offline methods. But, according to Zhang et al. [31]: *'However, the disadvantage of convex optimization is that the objective function and inequality constraint must be convex, and it yields limited applications.'* Therefore, convex solvers will not be discussed in further detail.
2. *Online methods:* online methods aim to optimize the cost function in real-time. According to Mustafa et al. [1] the different strategies that fall under this method are:

- (a) Equivalent consumption minimization strategy: According to Planakis et al. [2]: *'Equivalent consumption minimization strategy is a technique which considers the energy consumption of all the available power sources, scaled with a factor which represents the equivalent fuel consumption cost'*. Kalikatzarakis et al. [32] uses this method (or a more common variant, called Adaptive Equivalent consumption minimization strategy, which is explained below) by introducing a state variable  $s(t)$  that links fuel to electric energy consumption from the battery, therefore modelling the battery as if it were a fuel tank. One should take notice of the fact that the performance of an Equivalent consumption minimization strategy is closely tied to this aforementioned equivalence factor (or state variable) [33];
- i. Because of the impact of the equivalence factor, papers (such as Kalikatzarakis et al. [32], Xie et al. [34]) can be found that apply Adaptive ECMS. In this strategy, the equivalence factor is adjusted by certain states of the system.
- (b) Pontryagin's minimum principle: an analytical method of solving the optimization problem [35]. This method uses the principle of Hamiltonian mechanics to solve the optimization problem. Song et al. [30] has used the Pontryagin's minimum principle approach to minimize fuel consumption, but also maximize component lifetime. In the results, the author states that the Pontryagin's minimum principle has nearly the same optimal point as the offline optimization, indicating that the solutions from the Pontryagin's minimum principle are close to the true optimum whilst being applied in real-time.

The main advantage of the offline strategies is that the found minimum is the global minimum of the entire solution space, however as stated before, they are not able to do this in real-time. The advantage of the online methods is that they can find the optimal point in 'real-time', but the catch here is that the effectiveness of these strategies highly depends on chosen the co-states.

## 2.4. Machine Learning-based strategies

The essence of a learning-based method is to use offline optimization methods on a short-term horizon extending into the future [35]. This short-term horizon is predicted with methods such as model predictive control [27], stochastic dynamic programming [36] or Neural Networks [37]. the advantages of using Neural Networks are the high adaptive capacity [38], the robustness [38], and the low computational complexity when applied [15] The disadvantage of machine learning-based methods is the quantity and quality of the training data required [38], and the computational power that is necessary to train the model.

## 2.5. Health aware EMS

To become health aware, an EMS has to account for the current states of the components in the system and aim to minimize the overall impact of the EMS on power plant degradation Kandidayeni et al. [15] states that there are three ways to incorporate the health of the system:

- Prognostic: using a degradation model. Here the measurements of the different components are fed into a model that then estimates the state of those components. This predicts the remaining useful life (RUL) of the system based on its actual state of health (SOH);
- Diagnostic: monitoring the actual characteristics. This method tries to measure the state of the characteristics and tries to detect and isolate any faults before the system comes to a halt;
- Systematic: by considering different local control schemes. This method is more looking towards the battery management system or the Balance of plant (BOP) of the fuel cell.

If we look at how the literature approaches the health aware problem, Figure 2.2 shows that most research focuses on prognostic systems, and that there is a gap in the diagnostic health aware EMS's.

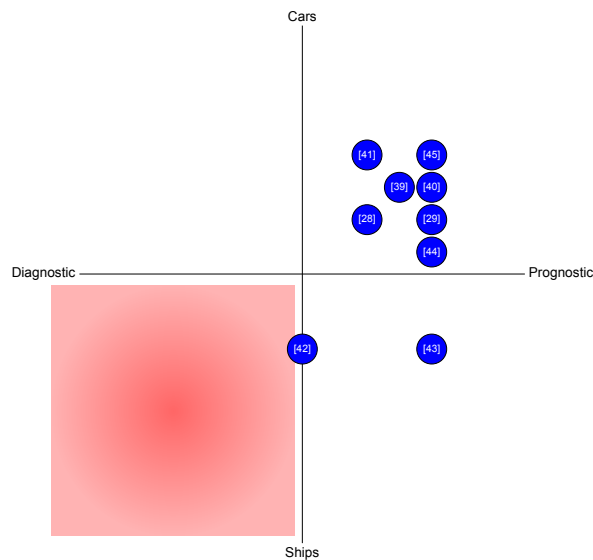


**Figure 2.2:** Distribution of prognostic and diagnostic health aware EMS

Additionally Figure B.1 in appendix Appendix B shows an overview of how different papers approach health-aware energy management. From this figure, the following conclusions can be drawn:

- The degradation of fuel cells is often described using fixed rates.
- Battery degradation is often described using empirical formulas
- Often the multi-objective problem is solved by finding a hydrogen consumption equivalent cost for degradation, which is based on the cost of hydrogen and the fuel cell/battery system. The danger of pre-determining the weights in the multi-objective problem is that the final result depends heavily on the chosen weights, whilst the costs might have changed over time.
- As the focus of the papers lies more on the health-awareness aspect, the used virtual models of the components are most often simplified to a basic formula.

## 2.6. Conclusion

From this chapter, it can be concluded that most health aware systems are still working from a prognostic viewpoint (based on the minimization of degradation models) even though Vermeer et al. [46] stated that: " *The presented review concludes that it is very difficult to generalize ageing behaviour (of batteries), concerning the effect of operational conditions.*" The same is true for the degradation of fuel cells, as there is even less information about the degradation behaviour. As the EMSs in literature aim to minimize the degradation caused by models, they have a chance of missing the actual degradation causes that are known and proven. The literature gap can be found in a health aware EMS for ships that will aim to work according to the diagnostic way. I.e. minimizing actual known causes of degradation instead of using models that aim to describe said behaviour, but are uncertain when it comes to actual component health simulation. The EMS in this thesis can then be benchmarked against literature and a not health aware EMS. More information about both of these will follow later in this thesis.

# 3

## Methodology

This chapter aims to present the framework for the EMS's by providing an overview of the ship in Section 3.1 and discussing the concept of the EMS in Section 3.2. After these sections, Section 3.3 and Section 3.4 contain an examination of the existing literature about the battery and the fuel cell degradation and virtual models respectively. These sections will also introduce the mathematical method behind the models used later in this thesis.

### 3.1. The ship

To obtain reliable results, data from the H2C boat [47] and a small fuel cell powered boat, are used to design the power plant component models and an accurate power profile that can be optimized. The power profile created by the data that is used for the optimization can be found in Figure 3.1a. The H2C boat is an initiative of the sailing innovation centre [47]. It is a lightweight RIB containing both a fuel cell and a battery. Resulting in the powerplant layout as in Figure 3.1b. The function of this R(H)IB is to show that it is possible to have a zero-emission coach boat for sailing teams in the Netherlands. It contains a 40 kWh Li-ion battery and an LT-PEMFC with an unknown power. These components create the power for the electric engine that is used as the propulsion of the ship.

The small fuel cell powered boat is from an unknown source. However it is known that the fuel cell itself is relatively small and does not have a large BOP. All problems related to a lack of data will be elaborated on in the next chapter. Whereas this chapter will focus on the methodology that will be used during this thesis.

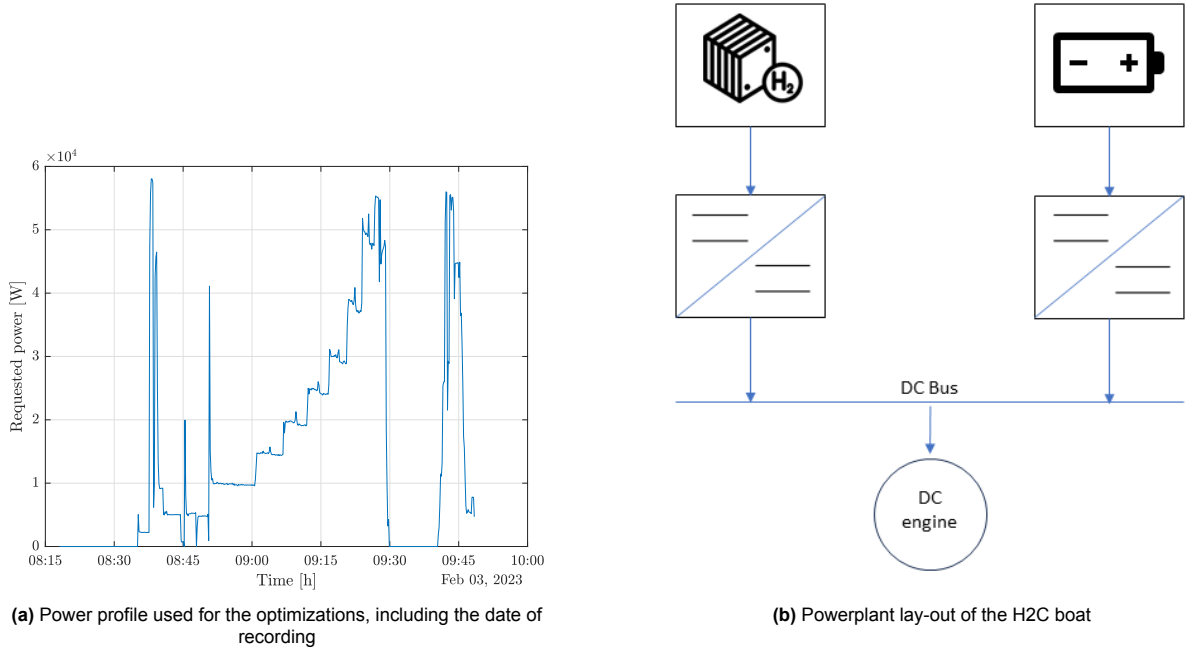


Figure 3.1: Validation of the degradation function with and without data

## 3.2. The health-awareness problem

Now that the case study (the H2C boat) is known, the framework for the EMS can be introduced. As stated in the previous section, the important power plant components that have to be modelled are a fuel cell and a battery. Because of limited time, the decision is made to focus on the components that generate or store power. For this reason, the DC-DC converters and the actual motor are not modelled. Since the EMS is responsible for delivering the requested power, this is considered representable. There are various approaches to designing a health aware EMS for this scenario. Most of the existing models focus on minimizing a function that describes the battery degradation corresponding with its operating conditions (i.e. a prognostic approach). However, this research will not minimize the degradation functions. Instead, it will aim to mitigate the actual causes of degradation. The discussed functions will provide the designed EMS with degradation feedback to accurately describe the behaviour of the battery and fuel cell. In other words, this research aims to simulate a diagnostic health-aware system. This cycle will repeat until either the battery has reached a total degradation of 20% or the fuel cell has reached a degradation of 0.1 V, which are the values where the power plants are seen as 'written off' [39, 40].

To accurately display the distinction between 'degradation feedback' and 'degradation minimization' on the basis of the functions, Figure 3.2 gives a schematic overview of the EMS framework that will be used later. Here the battery and fuel cell response systems give two types of feedback: the change in SOC, the hydrogen consumption ( $hydrogen_{cons}$ ) for time step  $\Delta t_i$  and the change in health (degradation) of the respective systems. The degradation caused by the decision in that time step  $\Delta t_i$  will be accumulated and saved. depending on the length of the power profile that will be used in the optimization, the actual degradation will be fed back to the power plant component models and their behaviour will be adjusted accordingly. The idea here, again, is that normally one would be able to measure the degradation of the components at a certain time step  $t = t_i$ , however as there is no access to a real 'online' system, the degradation feedback is handled like this. As will be discussed later, the EMS will then use this information to decide on the optimal control strategy.

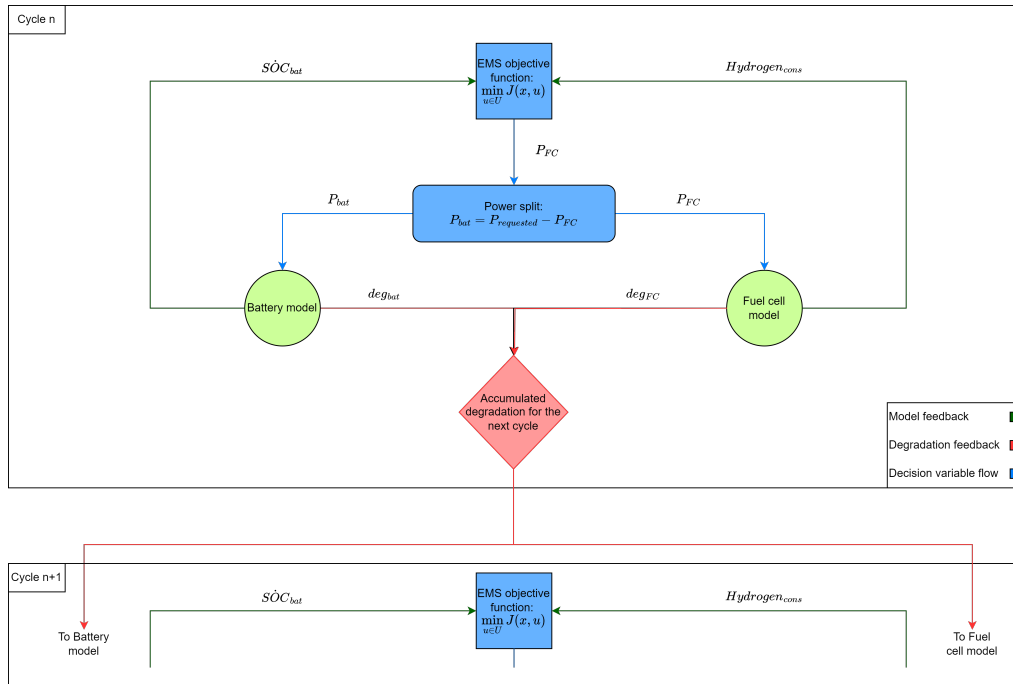


Figure 3.2: General idea behind the energy management system

### 3.3. Battery

This section gives a description of the battery model that is used in the optimization function. As can be seen in Figure 3.2, two variables are important in the EMS calculations: the change in the State Of Charge  $\dot{S}OC_{bat}$ , that gives feedback on how much of the total energy of the battery is left. And the degradation (or SOH), which relates to the degradation of the battery. The sections below will introduce the different models found in literature to estimate both these values.

#### 3.3.1. Change of State of Charge

Different methods to estimate the  $SOC$  exist [48]. One of the standardized and often used methods is Coulomb Counting. This method defines the  $SOC$  as:

$$SOC(t) = SOC(t_0) + \frac{1}{C_n} \int_{t_0}^{t_0+t} I_{bat}(d\tau) \cdot 100\% \quad (3.1)$$

In this equation, the most important parameters are battery capacity ( $C_n$ ) and the current through the battery ( $I_{bat}$ ). Lin et al. [36] simplifies this model to :

$$q(t) = SOC(t) = \frac{Q(t)}{C_n} \quad (3.2)$$

Where the current capacity ( $Q(t)$ ) is related to the battery capacity, which can be estimated by relating it to the drawn current using [2, 49, 50]:

$$\dot{S}OC = \frac{\eta_{bat} \cdot I_{bat}}{3600 \cdot C_n} \quad (3.3)$$

Here the battery efficiency ( $\eta_{Bat}$ ) represents the possible efficiency (and so the losses) in the battery whilst charging.

The big disadvantages of using this coulomb counting method are [51]:

- The initial  $SOC$  of the battery is required.
- The current sensors must be accurately calibrated.

- The maximum available capacity of the battery must be properly re-calibrated under various operating conditions and aging levels of the battery.

The first two are, for battery modelling, not the biggest problems as there is no 'real' current measurement and the initial *SOC* of the battery is an initial input parameter of the algorithm. The last requirement relates directly to the necessity for health-awareness, which will be introduced in Section 3.3.2.

The final unknown in Equation 3.3, is the current drawn from the battery for a certain requested power. This current can be calculated using an equivalent circuit model (ECM). Hu et al. [52], Lai et al. [53], He et al. [54] have compared different ECMs that can be applied to lithium-ion batteries, all authors agree that the first-order resistor-capacitor model (better known as the Thevenin model, as described by [55] and others) is the best choice considering computing complexity, accuracy and robustness. However, a disadvantage of this model is that it contains an algebraic loop, resulting in the addition of a discrete state that has to be remembered by the future EMS, resulting in a computationally more complex problem.

**Table 3.1:** EMS Battery models as found in literature

Citation	Battery aging?	Used equivalent circuit
[56]	No	Thevenin model
[55]	No	Thevenin model
[57]	No	Rint model
[32]	No	2nd order RC model
[58]	Yes	Rint model
[2]	No	Rint model
[59]	Yes	2nd order Rc model
[60]	Yes	Rint model
[61]	No	Rint model
[62]	No	Rint Model
[63]	No	Rint model
[64]	No	Rint model

Computationally simpler models do exist. According to Table 3.1 most health-aware EMS make use of the Rint model. As the computational load of the Rint model is smaller, without too much accuracy loss for the drawn current (according to [54], about 3 % of accuracy loss). For this reason, this research will apply this Rint model to estimate the drawn current from the battery.

#### Rint model

The ECM used for the Rint model assumes that the internal resistance in a battery can be described by a single resistor, resulting in the ECM as in Figure 3.3.

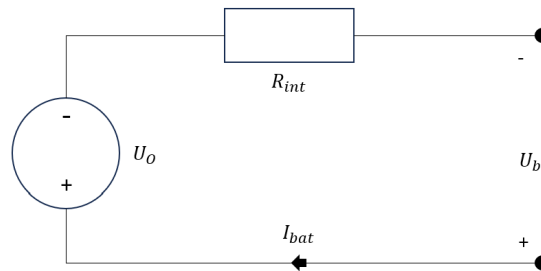


**Figure 3.3:** Rint model as found in Planakis et al. [2]

The link between the power drawn requested from the battery and the resulting current can be found using Kirchoffs law:

$$U_b = U_0 - i_{bat} \cdot R_{int} \quad (3.4a)$$

And we know that the  $P_{bat}$  is related to the current and voltage as:

$$P_{bat} = U_b \cdot i_{bat} \quad (3.4b)$$

Combining Equation 3.4a and Equation 3.4b results in [2, 50, 65]:

$$I_{bat} = \frac{U_0 - \sqrt{U_0^2 - 4 \cdot R_{int} \cdot P_{bat}}}{2 \cdot R_{int}} \quad (3.5)$$

Which can be combined with Equation 3.3 to get to the change in SOC:

$$S\dot{O}C_{bat(i)} = \frac{-U_{0(i)} + \sqrt{U_{0(i)}^2 - 4 \cdot (P_{req(i)} - P_{FC(i)}) \cdot R_{int}}}{2 \cdot R_{int} \cdot C_{bat}} \quad (3.6)$$

### 3.3.2. Battery degradation

As the degradation of the batteries is not covered in the previous section, this section explains different degradation causes and how they can be modelled and mitigated. Batteries degrade both due to physical stress and chemical side reactions during both cycling and idle states [46]. Three main ageing modes can be defined as responsible for lithium-ion battery degradation:

- Loss of Lithium Inventory: The loss of active lithium ions that are no longer available for cycling;
- Loss of Active Material: The loss or structural degradation of the available anode or cathode material;
- Conductivity Loss: Degradation of the electrical parts such as the current controller.

Particularly the loss of active material is interesting. According to Vermeer et al. [46], Safari et al. [66] and Barré et al. [67] the dominant factor causing this degradation, is the formation of a SEI layer on the negative electrode. This SEI layer is a layer that initially protects the electrode against solvent decomposition at large negative voltages, but over time it leads to a gradual capacity fade as the SEI layer thickens. [68].

The growth of this SEI layer (or the degradation of batteries in general) can be modelled in three different ways: Empirical / semi-empirical models, Physics-based models and Machine learning models.

This thesis focuses on the first, the empirical models, which are also often used in literature as can be seen in Figure B.1. The physics-based models as among others described in Safari et al. [66] are not used due to the computational complexity caused by multiple ODE describing the behaviour of a battery. Machine learning methods have the problem that they most often depend on lab data and according to Sui et al. [69] *‘[...] the SOH feature extracted from the lab data will be invalid as the battery may exhibit different degradation behaviour in real applications.’* And also need a lot of battery-related data, which is often not available.

#### Empirical models

Vermeer et al. [46] reviews multiple empirical models, and concludes that empirical formulae based on the Arrhenius equation times a time factor are the common used models when it comes to cycling or calendar ageing of batteries:

$$Q_{loss} = f(SoC, T, DOD, I) \cdot Ah^z \quad (3.7)$$

Wang et al. [6] claims that the depth of discharge (*DOD*) is not an influential factor if the discharge rate is low (below  $C/2$ ), which is most likely related to the fact that the *DOD* can then be described by using the current through the battery and *Ah*. The same author also uses the *Crate* of the battery instead of the discharge current *I* in Equation 3.7. Moreover, the value of *z* approaches 0.5, as the time-dependency of the solid electrolyte interphase (SEI) layer growth is a function of  $\sqrt{t}$  [70, 71]. Resulting in the empirical formula [6]:

$$Q_{loss} = B(C_{rate(t)}) \cdot \exp\left(\frac{-3700 + 370.3 \cdot C_{rate(t)}}{R \cdot T_{bat}}\right) \cdot Ah(t)^{0.55} [\%] \quad (3.8)$$

Here the  $T_{bat}$  will be assumed constant, and *R* has a value of 8.314. The pre-exponential factor *B* is difficult to quantitatively describe in relation to the discharge rate, however, Table 3.2 gives an overview of different *B*-values for different discharge rates. Finally *Ah*, "describes the net *Ah* delivered by the battery over multiple cycles" [46] or mathematically [6]:

$$Ah = Cycle\ number \cdot DOD \cdot Full\ cell\ capacity \quad (3.9)$$

**Table 3.2:** Generalized life models for certain c-rates as found in Wang et al. [6]

C-rate	C/2	2C	6C	10C
B-values	31630	21681	12934	15512

The disadvantage of this empirical model is that the function is discrete, not continuous and thus not true for all operating conditions i.e. 3C or capacity loss as a function of storage time. Next to that, it also not accounts for the loss of life during storage, due to the multiplication of the  $Ah$ , leading to zero capacity loss if the battery were to not be used. And finally, the model is built around the degradation of Li-FePO<sub>4</sub> batteries, other batteries are likely to follow different degradation patterns. Therefore, this model is only true in dynamic conditions where the battery will be used. If one is interested in models that do take a capacity loss in storage conditions into account, Ramasamy et al. [72] has proven (and modelled) capacity loss in the storage stage.

For now, Equation 3.8 gives sufficient feedback on the consequences of certain operating conditions as there are no better formulae found in the review literature. Therefore this formula will be used to describe the ageing of the battery present in this model.

## 3.4. Fuel cell

### 3.4.1. Virtual model

The second component is the fuel cell. For the fuel cell, two types of feedback are important: the SOH and the hydrogen consumption  $Hydrogen_{cons}$  over a given period  $\Delta t$ . This section will first introduce ways found in the literature to calculate the hydrogen consumption, after which it will go into the degradation of fuel cells.

Before going into the modelling of the fuel cell, first, a general understanding of fuel cells has to be made. Fuel cells generate electricity and heat via an electrochemical reaction, which is the reversed electrolysis reaction [73]. A fuel cell has five main parts: anode, cathode, electrolyte and/or membrane and an external circuit. Even though this layout is similar for nearly every fuel cell, different fuel cells operate on different fuel types and at different temperatures. The most common fuel cell types are [74]:

- Low-temperature proton exchange membrane fuel cells (LT-PEMFC);
- High-temperature proton exchange membrane fuel cells (HT-PEMFC);
- Alkaline fuel cell (AFC);
- Molten carbonate fuel cell (MCFC);
- Solid oxide Fuel cell (SOFC).

Each of these systems is controlled by a BOP. This system is responsible for water drainage, fuel cell cooling, fuel supply etc. And is assumed to be a perfectly operating unit that only draws a certain percentage of the energy generated by the fuel cell.

This section focuses on Low-temperature proton exchange membrane fuel cell (LT-PEMFC), which is the fuel cell type on board the H2C boat. For all fuel cells, the maximum electrical work obtained by a fuel cell at a constant temperature and pressure is given by the change in the Gibbs free energy change [3]:

$$\Delta G = -nFE_{rev} \quad (3.10)$$

Where F is Faradays constant (96,485 C/mol),  $E_{rev}$  is the ideal potential of the cell and  $n$  is the number of electrons in the reaction. The Gibbs free energy change can be rewritten as [3]:

$$\Delta G = \Delta G^0 + \frac{RT}{nF} \ln(Q_r) \quad (3.11)$$

Substituting Equation 3.10 in Equation 3.11 results in the general form of the Nernst equation [3]:

$$E_{nernst} = E^0(T_{reaction}) + \frac{RT_{reaction}}{nF} \ln(Q_r) \quad (3.12)$$

Where  $Q_r$  is the reaction quotient and  $T_{reaction}$  is the temperature of the reaction in kelvin,  $R$  is the gas constant and finally the  $E^0$ , which is equal to 1.18 volts at 298 K if the water products are in a gaseous state. This potential follows (for gaseous products) a linear downward trend for increasing temperatures [3].

This Nernst potential is the ideal potential of one cell. Impurities reduce this potential, and so will improper fuel consumption and other factors. However, the actual purity of the fuel is hard to estimate and will therefore be assumed pure in the rest of the research.

The reaction taking place in the anode of the PEMFC is [75]:



and at the cathode:



this means that the Nernst potential of a single cell PEMFC is equal to [3]:

$$E = E^0 + \frac{RT}{2F} \ln\left(\frac{P_{\text{H}_2}}{P_{\text{H}_2\text{O}}}\right) + \frac{RT}{2F} \ln(\sqrt{P_{\text{O}_2}}) \quad (3.15)$$

Where  $P$  is the relative (concerning the fuel cell pressure) gas pressure of each gas respectively, and  $P_{\text{H}_2\text{O}}$  is 1 due to the liquid phase of the generated water

Once this open circuit voltage (or Nernst potential) or the  $V_{0FC}$  is known, one can also calculate the delivered voltage of the fuel cell. This is done by taking an equivalent circuit with equivalent resistances. In many cases, the behaviour of these internal resistances of the fuel cell can be treated as linear in specific operating windows resulting in an Area Specific Resistance (ASR) [74]:

$$V_{cell} = V_{0FC} - I \cdot ASR \quad (3.16)$$

Figure 3.4 shows that if one were to assume neither a very low nor very high relative current density, Equation 3.16 holds. For this thesis this would mean that the fuel cell power is limited to:

$$P_{FC} \in [0.2...0.8] \cdot P_{FCmax} \quad (3.17)$$

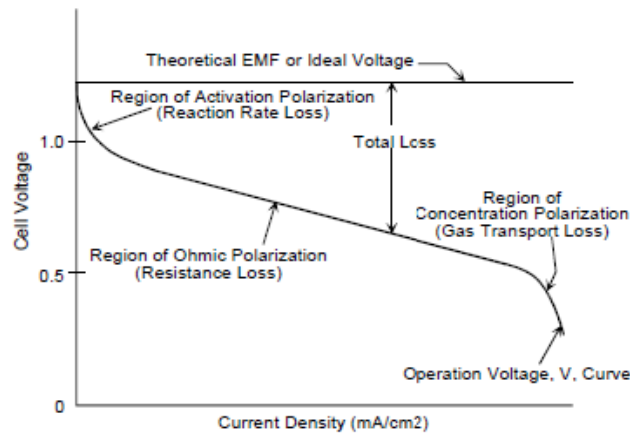


**Figure 3.4:** Ideal and Actual Fuel Cell Voltage according to Appleby and Foulkes [3]

The delivered power by the fuel cell is equal to:

$$P_{Stack} = I_{FC} \cdot V_{cell} \cdot N_{cells} \quad (3.18)$$

By combining Equation 3.16 and Equation 3.18 we can calculate the fuel cell current  $I_{FC}$ :

$$I_{FC} = \frac{-V_{OCVFC} \pm \sqrt{V_{OCVFC}^2 - 4 \cdot ASR \cdot P_{FC}}}{2 \cdot ASR} \quad (3.19)$$

Important here is that the final power delivered by the stack should also account for the power that the BOP consumes. To make estimations about the relation between the BOP consumed power and the power generated by the fuel cell, the linear relation found in Guzzella and Amstutz [76] can be used:

$$P_{aux} = P_0 + N \cdot k_{aux} \cdot I_{FC}(t) \quad (3.20)$$

This means that the final power delivered by the fuel cell would be equal to:

$$V_{OCVFC} \cdot I_{FC} \cdot N_{FC} - P_{aux} = P_{FC} \quad (3.21)$$

Where  $N_{FC}$  is the number of fuel cell cells. And finally, the relation between the requested power and the power through the fuel cell stack [76]:

$$I_{FC} = \frac{N_{FC} \cdot (V_{OCVFC} - k_{aux} - \sqrt{N_{FC}^2 \cdot (V_{OCVFC} - k_{aux})^2 - 4 \cdot N_{FC} \cdot ASR \cdot (P_{req}(t) + P_0)}}{2 \cdot N_{FC} \cdot ASR} \quad (3.22)$$

Once the drawn current by the fuel cell is known, we can estimate the hydrogen consumption by the fuel cell. This is because of the relation between the number of electrons and hydrogen atoms as described in the reaction equation in Equation 3.13. So for each electron, we need a hydrogen particle. The capacity of 1 Mol of electrons is 96485 Coulomb (F).  $1 \text{ A} = 1 \frac{\text{C}}{\text{s}}$ , thus:

$$H_{2,cons \text{ mol}} = \frac{I_{FC} \cdot N_{cells}}{2 \cdot F} \cdot \Delta t \text{ [mol]} \quad (3.23)$$

By multiplying this hydrogen consumption with the molar mass of hydrogen, we get the consumption in grams:

$$H_{2,cons \text{ grams}} = H_{2,cons \text{ mol}} \cdot 1.00794 \quad (3.24)$$

The above is assuming 100 % hydrogen conversion. Which, is due to hydrogen crossover through the membrane [77] not necessarily true. Interestingly is, this hydrogen crossover enlarges as the fuel cell ages [77] and thus makes the fuel cell less and less efficient.

The final important factor of the fuel cell is the efficiency of the system. As we still assume that the total hydrogen conversion is equal to 100 %, we can start by calculating the ideal efficiency of the fuel cell, which is equal to [3]:

$$\eta_{ideal} = \frac{\Delta G}{\Delta H} \quad (3.25)$$

Where  $\Delta G$  is the change of Gibbs free energy, and  $\Delta H$  is the change in enthalpy of the reaction inside the fuel cell, which can be found by combining Equation 3.13 and Equation 3.14:



From this, at standard conditions (25°C, 1 atm),  $\Delta H$  is equal to 285.8 kJ/mol (higher heating value of hydrogen) and  $\Delta G$  is equal to 237.1 kJ/mol, therefor the ideal efficiency is equal to:

$$\eta_{ideal} = \frac{237.1}{285.8} \approx 0.83 \quad (3.27)$$

Using this ideal efficiency, we can calculate the Higher heating value efficiency of the fuel cell system [3]:

$$\eta = \frac{\text{Usefullenergy}}{\Delta H} = \frac{V_{actual} \cdot \text{current}}{(V_{ideal} \cdot \text{current})/0.83} = \frac{0.83 \cdot V_{actual}}{E_{ideal}} \quad (3.28)$$

Where it is assumed that  $\Delta H = 0.83 \cdot \Delta G$  and  $\Delta G = V_{ideal} \cdot \text{Current}$ . According to Appleby and Foulkes [3]: "the ideal voltage of a cell operating reversibly on pure hydrogen and oxygen at 1 atm pressure and 25°C is 1.229 V." Thus the efficiency of the system is equal to [3]:

$$\eta = \frac{0.83 \cdot V_{cell}}{1.229} = 0.675 \cdot V_{cell} \quad (3.29)$$

Often referred to as the voltage efficiency of the fuel cell.

### 3.4.2. Fuel cell Degradation

PEMFCs degrade due to several causes, as can be found in Table 3.3. But, not all components of the fuel cell have the same influence on the overall usage. The degradation of membrane and electrodes inside the fuel cell has more influence on the overall reduction of the RUL than the other components [78]. The main contributors to the degradation of the membrane and electrodes can be summarised

**Table 3.3:** Most common degradation causes for fuel cells according to literature

citation	type	component	Degradation causes
van Biert and Visser [74] De Bruijn et al. [79] Wu et al. [80]	LT-PEMFC PEMFC LT-PEMFC	Bipolar plate Bipolar plate Bi-polar plate	poisoning of the fuel due to release of its particles corrosion due to the aggressive acidic and humid environment inside a PEM fuel cell,
van Biert and Visser [74]	LT-PEMFC	Catalyst and fuel electrodes	Fuel impurities, especially Carbon dioxide (or carbon monoxide)
Wu et al. [80]	LT-PEMFC	Catalysts	Electrochemical degradation due to the formation of HO and HOO that attacks the membrane chemically
Wu et al. [80]	LT-PEMFC	Catalysts	Carbon corrosion due to transitioning between startup and shut-down cycle and fuel starvation due to the blockage of $H_2$ from a portion of the anode. The second is caused by high overall stack utilization
De Bruijn et al. [79]	PEMFC	Electrodes	Potential cycling, elevated temperature, relative humidity start stop cycles and fuel starvation and carbon corrosion due to the start stop cycles
Wu et al. [80] Wu et al. [80]	LT-PEMFC LT-PEMFC	Gas diffusion layer Membrane	mechanical degradation, caused by swelling of the membrane in wet conditions and contracting of the membrane in dryer conditions.
Wu et al. [80] Wu et al. [80]	LT-PEMFC LT-PEMFC	Membrane Membrane	Thermal degradation, caused by rapid startup Electrochemical degradation due to the formation of HO and HOO that attacks the membrane chemically
van Biert and Visser [74]	LT-PEMFC	Membrane	Dehydration of the membrane gives a reduction in ionic conductivity.
van Biert and Visser [74] De Bruijn et al. [79] Wu et al. [80]	LT-PEMFC PEMFC LT-PEMFC	Membrane Membrane Sealing gasket	poisoning due to Ammonia Cycling of voltage, humidity and temperature The corrosive environment that also destroys the membrane, is also responsible for the corrosion and degradation of the sealing gaskets, which could lead to spillage between fuel cells in the stack.

in the loss of electrochemically active surface area in the catalyst layer of the fuel cell. Other types of degradation have been discussed in De Bruijn et al. [79], Wu et al. [80].

Both De Bruijn et al. [79], Wu et al. [80] mention that the degradation rates of PEMFC increase with load cycles, start-stop cycles and fuel starvation. During the start-stop cycle, the main factor causing electrochemical active surface area degradation is reactant starvation [28]. During the other, high-potential operational conditions, the main degrading factor is carbon corrosion [28]. In the PEMFC the most occurring catalyst is platinum nano-particles supported by carbon atoms [81]. As the carbon that supports the platinum nano-particles becomes unstable and starts oxidizing in hotter operating conditions, Platinum particles can start to dissolve due to the formation of and reaction with  $\beta$ -oxides. Once the particles are dissolved, De Bruijn et al. [79] states that Ostwald ripening and the aforementioned carbon corrosion affect the Pt particle growth. Wu et al. [80] Does not fully agree with De Bruijn et al. and states that: *'However, so far, there is still no agreement on which mechanism is dominantly responsible for the catalyst particle growth'*.

Finally, Zhao et al. [81] also concludes that even though the carbon corrosion is way higher during startup and start down of the Fuel cell, the accumulated corrosion over time due to the fuel cell being operated is also a notable degradation factor.

The degradation rates for certain operational conditions (regardless of the actual cause) have been analysed by multiple papers, which have been reviewed in De Bruijn et al. [79], Wu et al. [80]. Chen et al. [82] tests a Fuel cell under dynamic loading conditions and relates the lost voltage to those dynamic conditions. Similar research (on the same data even) was carried out by Pei et al. [83], their findings are concluded in Table 3.4.

**Table 3.4:** Degradation rates PEMFC

Cycle	Chen et al. [82]	Pei et al. [83]
Start-stop [ $\frac{V}{cycle}$ ]	0.00197 %	0.00196 %
Idling [ $\frac{V}{h}$ ]	0.00124 %	0.00126 %
Load change [ $\frac{V \cdot kW}{cycle}$ ]	0.00006%	0.000059 %
High power load [ $\frac{V}{h}$ ]	0.00143 %	0.00147 %

Even though the displayed information comes from the same data, the authors represent their data with a slight difference. The results in the paper of Chen et al. have been presented as absolute values, where Pei et al. presents percentages. During the calculation from absolute values to percentages, very small rounding errors could have caused this slight difference in results.

The percentages corresponding to each degradation step can be utilized to determine the actual voltage loss. For both research papers, especially the loss during idling conditions is interesting, as that can be compared to other results. Both idling conditions result in a loss of  $8.82\mu V$  per hour. This is within the proposed range of  $2 - 10 \mu V$  found in [80] and is close to the average of  $6\mu V$  found in [79]. Therefore these four papers agree on the losses of idle usage of a fuel cell.

What is missing in the papers of [82] is the size of the fuel cell. One can calculate back to the original potentials of the fuel cell by looking at the potential at ( $t=0$ ), but the actual original information of the fuel cell is unknown. Additionally, the author does not mention the definition of the states (what loading of the fuel cell is an idling condition, what is a load change condition etc.). Pei et al. [83] Does give these conditions:

- Start-stop cycling: from cold to 1 minute at  $10 \frac{mA}{cm^2}$  back to the cold status.
- Idling condition: constant load of  $10 \frac{mA}{cm^2}$ .
- Load changing operation: from idling to rated power condition.
- High power load cycling: loading according to the limited voltage in the fuel cell bus.

### 3.5. Conclusion

This chapter introduced the use case and the general idea behind the EMS. This thesis will focus on bench-marking a diagnostic health aware EMS against a not health aware EMS and a health aware EMS found in the literature. The different models that are used to describe the virtual power plants in state-of-the-art literature have been introduced. Concluding that the  $R_{int}$  model will be used to describe battery behaviour and a similar, constant resistance model will be introduced to describe the behaviour of a fuel cell. Finally, the degradation for both components has also been introduced, which showed that even the current solutions can still not fully capture the degradation behaviour of either a fuel cell or a battery.

# 4

## The EMS Functions

This chapter gives an overview of the mathematical equations and models that are used by the DP solver introduced in Chapter 3. Each function corresponds to Figure 3.2, where the actual cost function is the only thing that changes for each system. This chapter first introduces the data-based battery and fuel cell model in Section 4.1 and Section 4.2. The following sections describe the mathematical description of the health and not-health aware cost functions.

### 4.1. Battery model

To get an accurate estimation of the energy consumed by the battery, the discussed functions in Section 3.3 can be used. However, to get a digital twin of the components, one has to fit the functions for  $\dot{SOC}_{bat}$  (Equation 3.6) to the data provided. To do this, an algorithm that can fit equations to data has been applied to the data, where the data has been split into a training and a validation sample.

#### 4.1.1. Fitting and validation $R_{int}$ model

From the operating data of the H2C boat, different plots about the behaviour of the ship can be made. If this data were to be fitted to Equations 3.3-3.6, using a training and validation split, one can find different the parameters necessary to describe the behaviour of the battery:

##### Battery pack capacity

To obtain  $Q_0$ , Equation 3.3 can be used which shows that the change of  $SOC$  is a function  $SOC$  is a function of the current at that moment, divided by the capacity of the battery. Plotting the current against the change of  $SOC$  results in a battery pack capacity of 108  $Ahr$

##### Internal resistance

The internal battery resistance  $R_{int}$  of the battery pack on board the H2C boat can be calculated by assuming a constant  $V_{OCV}$ . This means that:

$$P_{bat} = V_{OCV} \cdot I_{bat} - I_{bat}^2 \cdot R_{int} \quad (4.1)$$

By fitting the delivered battery power to the current drawn by the battery, we can fit the constant  $V_{OCV}$  and the internal battery resistance  $R_{int}$ , which results in an internal resistance of  $1.86 \cdot 10^{-1} \Omega$ .

##### Relation between $V_{ocv}$ and $SOC$

The actual  $U_{OCV}$  decreases as the  $SOC$  decreases. Figure 4.1 is an example of what such a relation would look like. By assuming that the relation between the  $SOC$  and  $U_{OCV}$  is linear in the interval between 20 – 80%  $SOC$ , one can find the relation between these two in the H2C data. If done one finds:  $V_{OCV} = 75.6 \cdot (\frac{SOC}{100}) + 310$ , which combined with the found battery pack capacity in  $Ahr$  results in a fully charged battery capacity in  $kWh$  of  $\approx 41$ , which is about equal to the 40 kWh as stated in Section 3.1

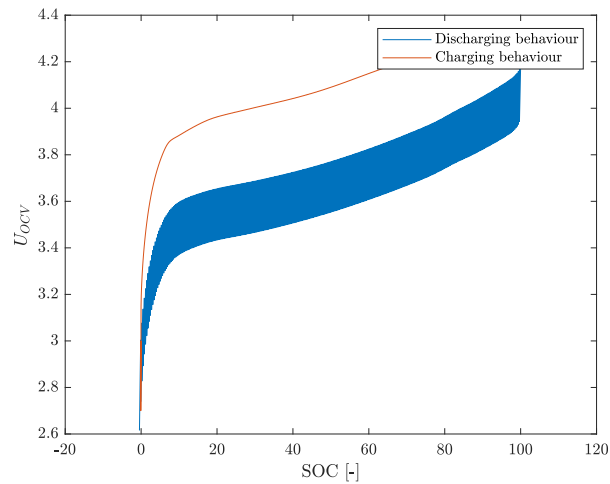
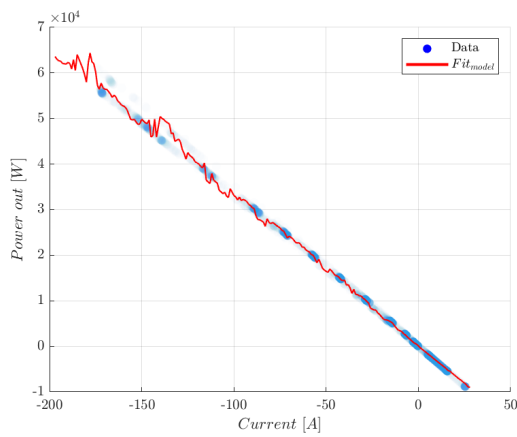


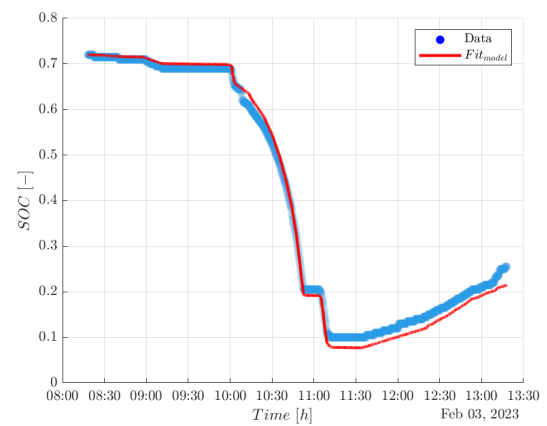
**Figure 4.1:** Charging and discharging behaviour of a battery, data retrieved from McIntosh [4]

## Results

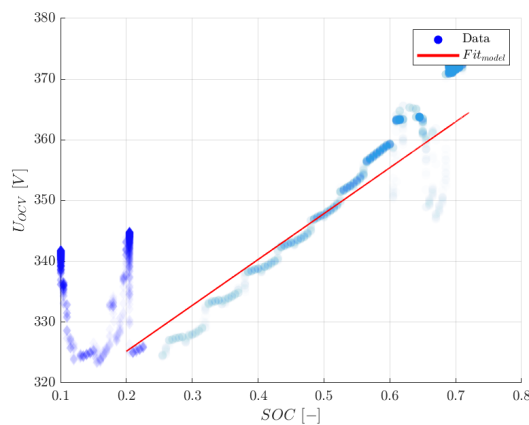
Using the parameters as discussed above, the produced battery model has been simulated using the data of the H2C boat, resulting in Figure 4.2.



**(a)** Current power relation of the H2C battery



**(b)** SOC of the battery over time, simulated using power demand from the H2C boat



**(c)** relation between  $U_{OCV}$  and  $SOC$

**Figure 4.2:** Comparison of the behaviour of the  $SOC$ ,  $I_{bat}$  and  $U_{OCV}$

Where the respective MAPEs for these figures are:

- Figure 4.2a: 0.99%, this error is within the acceptable margins and is mostly caused by averaging the fitted data, as there are multiple points with the same output power, but a different  $SOC$  and thus a different  $U_{OCV}$ , resulting in a different current.
- Figure 4.2b: 8.33%, one can see that over time, the error in the  $SOC$  seems to deviate more and more from the original data. The change in  $SOC$  also accumulates all the errors and assumptions of the model, therefore, especially at the end of the simulation the accumulated error becomes noticeable. As the  $SOC$  on the battery gets reset after each iteration, the error will never become larger.
- Figure 4.2c: 4.36%, which is mostly caused by the linear estimation of the  $U_{OCV}$ , as the behaviour can also be described by higher order equations. For this thesis, however, this model can be seen as feasible as it is often used in comparable literature.

Interestingly is that in Figure 4.2c the  $U_{OCV}$  seems to increase at the low  $SOC$ , these points are also marked by squares. This can be explained by the charging behaviour of a battery caused by hysteresis, as can also be seen in Mamyrbayeva et al. [84]. Charging a battery will cost more power than the power that can be gained by discharging the battery. This is normally solved by giving a value  $< 1$  to the  $\eta_{bat}$  (see Equation 3.3) as done in Bassam et al. [63], Song et al. [85], Pivetta et al. [86]. However, the effects are only small and are normally handled by the battery management system. It will therefore not have a big effect on the degradation of the components, especially because the discharge rate has to be rounded to the values as discussed in Table 3.2. Therefore, this thesis will neglect the effects of hysteresis and has also not used these points in the training of the model.

#### 4.1.2. Degradation Validation

As the degradation is not part of the data gathered by the H2C boat, the degradation function is tested against the data gathered by McIntosh [4], which contains data about the capacity fade of a battery cell. This means that the battery parameters in the model are to be adjusted to model the battery cells used in McIntosh [4].

Section 3.3.2 concluded that Equation 3.8 will be used to describe battery degradation. Equation 3.8 contains two problems that have to be solved before it can be used in this thesis.

1. The  $Ah$  is the total Ampere-hours of throughput through the battery. This means that the battery degradation can only be calculated after a certain period using the rain flow method, as done in [43, 87, 88].
2. The function only describes the degradation of a battery that is loaded constantly over its lifetime, so there is a fixed C-rate over the battery lifetime.

An alternative approach to solving problem 1 involves employing discretization techniques to get a  $\Delta Q_{loss}$ . Perez et al. [89] does so by stating a maximum percentage loss  $\Delta Q_{loss}$ . From there the author derives the maximal allowable throughput in ampere-hours and the number of cycles corresponding to that maximal allowable throughput. This gives a big disadvantage: the function depends on the maximum allowable cycles of the battery and is closely related to the maximal degradation of 20 %. For a more detailed explanation of this derivation, please refer to [89].

Due to the disadvantage described above, this thesis derives a different approach to discretize this problem. As can be seen in Equation 3.9, the ampere-hours consist of three parts:

- The cycle number ( $n_{cycle}$ ).
- The DOD of the battery in that cycle.
- The total cell capacity.

This means that the equation can be rewritten as:

$$Ah = 2 \cdot n \cdot \frac{I_{cycle} \cdot t_{cycle}}{C_{bat}} \cdot C_{bat} = 2 \cdot \sum_{i=1}^{i=n} I_{cycle(i)} \cdot t_{cycle(i)} = \frac{2 \cdot I_{bat} \cdot t}{3600} \quad (4.2)$$

Where the entire derivation has to be multiplied with 2, in accordance with Perez et al. [89], so that the charging is also included, as the original  $Ah$  only looks at discharging. If this function for  $Ah$  is

discretized over time, we can take the derivative of the capacity fade over time to obtain the degradation step due to certain operating decisions:

$$\frac{\Delta Q_{loss}}{\Delta t} = \frac{B(C_{rate}(t)) \cdot \exp\left(\frac{-3700+370.3 \cdot C_{rate}(t)}{RT}\right)}{\Delta t} \cdot \frac{\Delta\left(\frac{2 \cdot I_{bat} \cdot t}{3600}\right)^{0.55}}{\Delta t} \quad (4.3)$$

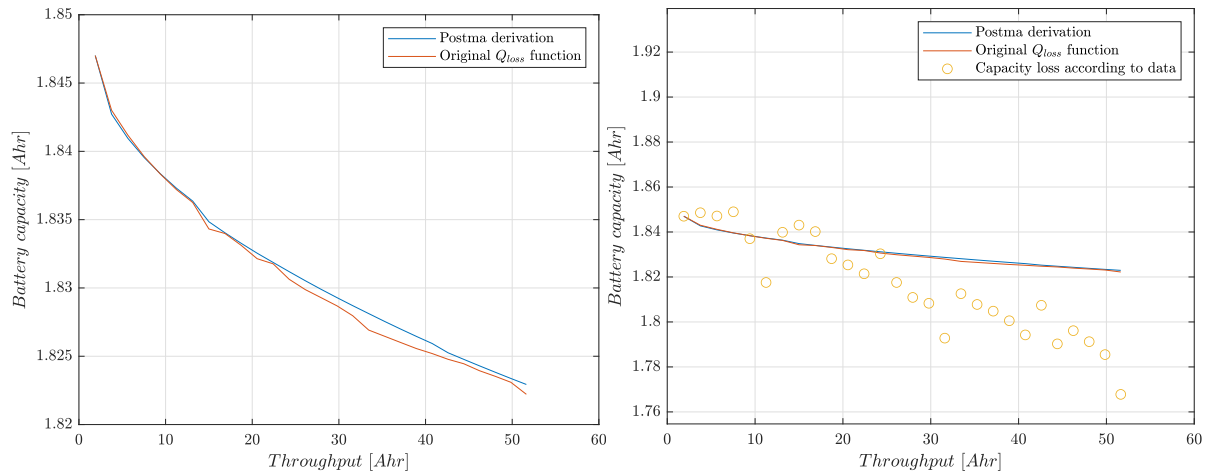
It is assumed that at an instant  $t$ ,  $I_{bat}$  is constant, which makes  $I_{bat}$ ,  $C_{rate}$  and  $B$  constant over timestep  $\Delta t$ . Therefore only the accumulated Ampere hours are a function dependent on time. Differentiating that results in:

$$\frac{\Delta\left(\frac{2 \cdot I_{bat} \cdot t}{3600}\right)^{0.55}}{\Delta t} = \frac{0.008911746244 \cdot I_b}{(I_b \cdot t)^{0.45}} \quad (4.4)$$

resulting in an increase in a percentage loss equal to:

$$\Delta Q_{loss} = \Delta B(C_{rate}(t)) \cdot \exp\left(\frac{-3700 + 370.3 \cdot C_{rate}(t)}{RT}\right) \cdot \frac{8,9e-3 \cdot I_b}{(I_b \cdot t)^{0.45}} \cdot \Delta t \quad (4.5)$$

For comparison, the original function (Equation 3.8) and the derived function (Equation 4.5) have been applied on the data found in McIntosh [4], resulting in Figure 4.3a



(a) Relation between Equation 4.5 and Equation 3.8 tested on data from (b) Validation of Equation 4.5 and Equation 3.8 on data from McIntosh [4]

**Figure 4.3:** Validation of the degradation function with and without data

As demonstrated in Figure 4.3a, Equation 4.5 exhibits an accurate fit with the original function. However, upon plotting the measured degeneration data found in McIntosh [4] as done in Figure 4.3b, another drawback of Equation 3.8 becomes evident. Namely, the disparity between the data points and the modelled degradation.

Three potential factors could have contributed to this behaviour:

- Firstly, it is the original function is based on graphite  $\text{LiFePO}_4$  batteries, while the measured data corresponds to an unknown type of Li-ion batteries. If these battery types are not identical, it could lead to variations in degradation behaviour.
- Secondly, the conditions of both experiments, apart from temperature, remain unknown. It is possible that other factors, such as cycling protocols, charging rates, or electrolyte compositions, may have influenced battery degradation, resulting in disparate degradation measurements.
- Thirdly, the absence of information regarding the accuracy of the measurement equipment introduces the possibility of error accumulation over time, potentially yielding divergent results.

One could choose to try and fit Equation 4.5 parameters to the degradation data as displayed in Figure 4.3b, however, the batteries of the H2C boat are likely to be of a different type than the data from [4] and the batteries that were used to design the original function, therefore the parameters as found in Equation 4.5 are kept for the model used in this thesis.

Finally, for this thesis, no cooling solution for the battery has been modelled. As there is no cooling solution, the temperature of the batteries can not be calculated. Therefore a constant battery temperature of 15 degrees has been taken, which is based on the average temperature of the north sea (14 degrees) and some efficiency losses. Even though this temperature is quite low, it also allows for a longer powerplant lifetime, which might enlarge the differences between the EMS's

## 4.2. Fuel cell model

In this section, the methodology will be applied to get an actual fuel cell model. As stated before, even though there is an availability of data on a fuel cell, it is not the fuel cell that is located on the H2C boat, this introduces several estimations that have to be made about the fuel cell behaviour. In the following sections, the necessary steps to calculate the hydrogen consumption and *SOH* of the fuel cell will be explained. The data considered contained information of a single 48-cell stack, able to deliver a maximum of 1200 watts of power.

### 4.2.1. Validation of the virtual model

To ensure that the formulae presented in Section 3.4.1 hold, the following assumptions are considered:

1. The power range of the fuel cell should be as described in Equation 3.17.
2. The resistance losses in the fuel cell are assumed to be linear with respect to the current, as described in van Biert and Visser [74].
3. The relationship between  $U_{FC}$  and  $U_{OCV}$  can be expressed by the equation  $U_{FC} = U_{OCV} - (k_1 - R \cdot I)$ . The polarization losses, outside the range described in Equation 3.17, are described by the difference between  $E^0$  and  $U_{OCV}$ , which is commonly referred to as the voltage efficiency of the fuel cell.
4. The fuel cell will have a hydrogen conversion of 100 %. Meaning that 100 % of the fuel is converted to energy. In reality, this number is lower than 100 %

To get an accurate model describing the fuel cell behaviour, there are several important parameters:

1.  $V_0FC$  and  $E^0$  relation.
2.  $U_{FC}$  and  $V_0FC$  relation.
3.  $K_{aux}$  and  $P_0$  of the BOP of the fuel cell.

#### $V_0FC$ and $E^0$ relation

The relation between the actual open circuit voltage of the fuel cell and the standard potential is described in Equation 3.12. Even though the measurements of the fuel cell do show a respective temperature, they do not show the information required to estimate the reaction quotient  $Q_r$ . As this estimation is also quite hard to make accurately, this model assumes that the  $V_0FC$  is the fuel cell voltage when the drawn current is  $\approx 20\%$  of  $I_{max}$ . This will then also include the polarization losses that occur in the region of  $1..20\%$  of  $I_{max}$

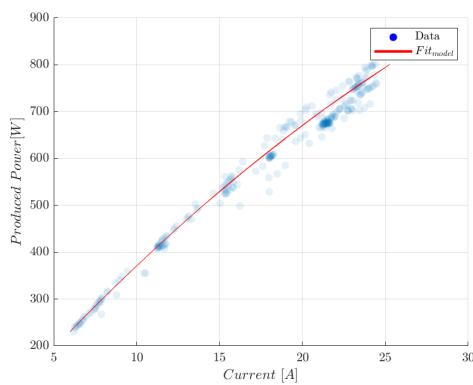
#### $U_{FC}$ and $V_0FC$ relation.

As there is information about the actual voltage delivered by the stack at different currents, one can estimate both the value for  $V_0FC$  and  $U_{FC}$ . Equation 3.16 shows that one can assume a linear relationship between these two, as there is a constant internal resistance. If done so, one can find that the  $V_0FC$  of a single cell is  $\approx 0.8$  at 20% load. Which corresponds with open circuit voltages at 20 % of the maximal current as found in Grasser and Rufer [90], Musio et al. [91]

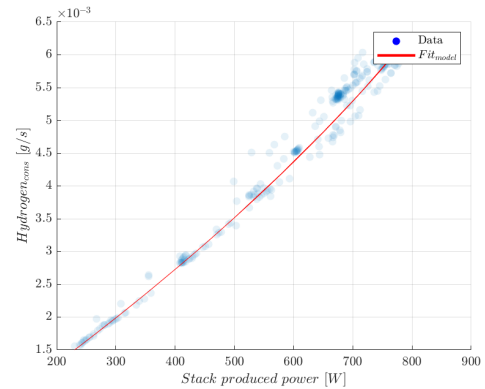
Before continuing to the calculations made on the BOP, Figure 4.4 contains the results of the model thus far. As can be seen, the model fits the data quite accurately, only resulting in a MAPE (per sub-figure) of:

- Figure 4.4a: 3.59 %.
- Figure 4.4b: 3.76 %.
- Figure 4.4c: 3.76 %.

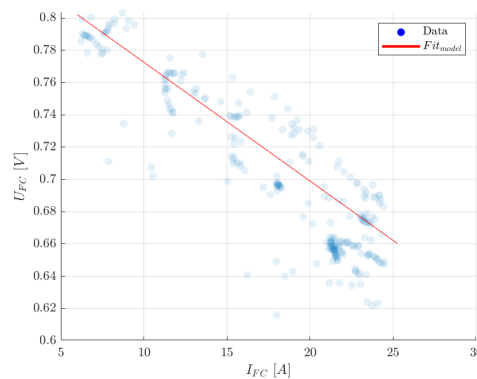
These numbers are hard to compare to literature, however, a cause can be the large spread of  $U_{FC}$ , which can be caused by load changes on the fuel cell, resulting in a less efficient reaction during the transitional phase and so a lower open cell voltage, and thus a different  $U_{FC}$  for the same current. However Figure 4.4 combined with these MAPEs show that there is a good fit with the data.



(a) Relation between stack power and stack current



(b) Relation between stack produced power and hydrogen consumption



(c) relation between  $U_{FC}$  and fuel cell current

**Figure 4.4:** Comparison of the power current, power hydrogen consumption and voltage-current relation of the fuel cell

BOP:

The fuel cell data does not contain any information about the BOP. This is mostly because of the small size of the fuel cell stack, resulting in only minimal energy consumption of the fuel cell stack. However, the maximum power requested by the H2C electric motor is 60 kW. Given the maximum power contribution of the fuel cell to the power output, we assume that the fuel cell has 40, 48-cell stacks. A fuel cell of this size, however, will have to lose power to the BOP for the transport of water, cooling etc. of the entire fuel cell power plant. Therefore assumptions have to be made about the effects of the BOP on a single stack. Therefore the  $k_{aux}$  and  $P_0$  have been iterated until a maximum efficiency of about 53% has been found, which is about the maximum efficiency of small-size fuel cells as found in Figure 4.5.

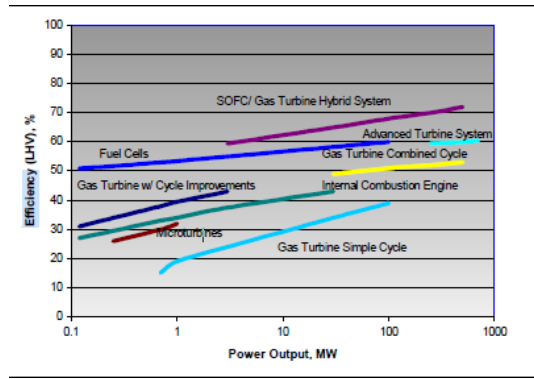


Figure 4.5: Efficiency of different systems according to Appleby and Foulkes [3]

This results in a respective value of  $0.55 W$  for  $P_0$  and a value of  $0.15 V$  for a single cell, or about  $1000 W$  for  $P_0$  and a value of  $6V k_{aux}$  for the entire system. Combining these results gives the fuel cell results including BOP as in Figure 4.6:

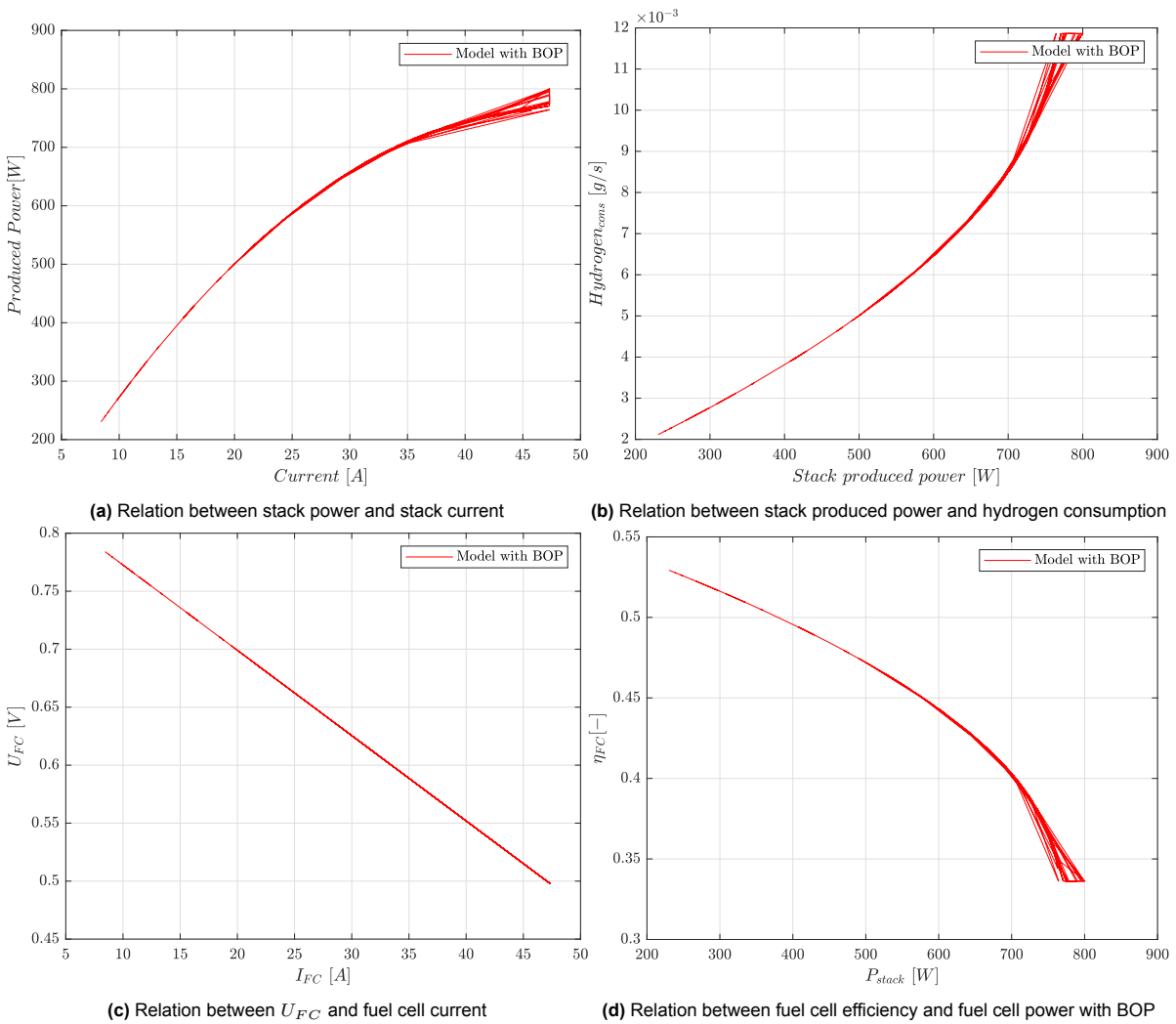


Figure 4.6: Comparison of the power current, power hydrogen consumption and voltage-current relation of the fuel cell with a BOP

### Fuel cell degradation

As it is not possible to compare or validate the degradation model with actual data, the values shown in Table 3.3 have been translated to have the same degradation characteristics as described in Fletcher et al. [39], except for the idling degradation rate, which is based on the percentages found in Table 3.3 and scaled to a (constant) open circuit voltage of 0.9, which is based on the fact that the actual open circuit voltage should be slightly higher than the open circuit voltage found in the previous subsection. Doing so results in Table 4.1:

**Table 4.1:** Applied degradation rates for the fuel cell system

Cause	Effect
start stop	-2.39E-05 V
idling	-1.02E-05 V/h
load change	-4.41E-11 V/ $\Delta W$
high power load	-1.17E-05 V/h

## 4.3. Not health-aware EMS

The not-health-aware EMS will both serve as a benchmark and as a basis for the health-aware function. Certain assumptions and all constraints will automatically transfer over to the other functions. As there is a high likelihood of the problem being solved discrete, the general equation for the not health aware EMS becomes:

$$\min_{u \in \mathbb{R}} \sum_{i=1}^{N-1} J(x, u) \quad (4.6)$$

For the not health-aware objective function, the objective is to consume the least hydrogen possible, which is a function of the fuel cell power. If we also were to assume that there will never be an energy surplus (the total used energy is never larger or smaller than the required power), the following assumption, which is also used in Hu et al. [20], Ouddah et al. [92], Ansarey et al. [93] will hold

$$P_{bat}(i) = P_{req}(i) - P_{FC}(i) \quad (4.7)$$

The decision variable  $u$  can then be made equal to  $P_{FC}$  and the state variable  $x$  equal to the hydrogen consumption. combining this with Equation 3.6 results in the total, not health-aware energy management function:

$$\begin{aligned} & \min_{u \in \mathbb{R}} \sum_{i=1}^{N-1} J(x, u) \\ \text{s.t.} & \\ & J(x) = E_{H_2} = \sum_{i=0}^{N-1} f(P_{FC}(i)) \cdot \Delta T_i \end{aligned} \quad (4.8)$$

### 4.3.1. Constraints

To simulate a realistic loading scenario, constraints are required for the system. These can be quantitative constraints on the state of the components, but also the time step should be taken into account. This subsection elaborates on each chosen constraint.

**Constraint 1** *Limit the SOC between 20%..80%:* For the Rint model to be hold, the *SOC* should be limited between [20%..80%], thus:

$$SOC \in [20, 80] \quad (4.9)$$

**Constraint 2** *Limit the maximum power change on the fuel cell:* Fares et al. [57] considers a maximal allowable load change on the fuel cell of  $\approx [14. - 14] \% \frac{1}{s}$  in his EMS. This is also considered as the maximum allowable load change on the fuel cell in this thesis. However, this is only true if the fuel cell is on, so if the fuel cell power in the previous time step is zero, this constraint does not apply.

$$\Delta P_{FC} \in \begin{cases} -\text{inf}, \text{inf} & P_{FC}(i-1) = 0 \\ 0.14, -0.14 & P_{FC}(i-1) \neq 0 \end{cases} \quad (4.10)$$

**Constraint 3** Limit the current of the fuel cell between 20%, 80% of the maximum current. Equation 3.16 requires the maximum power requested from the fuel cell to be between 20 and 80. This will be done by limiting the power through the fuel cell:

$$P_{FC} \in [0.2, 0.8] * P_{FC(\max)} \quad (4.11)$$

**Constraint 4** Set the initial SOC for the battery. An initial SOC for the battery is necessary. For this thesis, this will be set to 0.5. Due to the size of the battery, a higher SOC would result in a decrease of the work done by the fuel cell, and a lower SOC would create an unfeasible scenario, as the fuel cell cannot generate enough power to sustain the power cycle on its own. The SOC will be reset for each iteration, assuming that the battery gets charged after each cycle:

$$SOC(t_0(k)) = 0.5 \quad (4.12)$$

**Constraint 5** Set the initial degradation of both the fuel cell and the Battery. The initial degradation for the battery is zero. Important note is that instead of using  $t_0(k)$  as in Equation 4.12, here we will use  $t_0$ , as the degradation is not be reset each iteration:

$$SOH(t_0) = 0 \quad (4.13)$$

**Constraint 6** Limit the maximal allowable power change per second on the fuel cell. Fares et al. [57] uses a maximal allowable load change on the fuel cell of  $\approx [14, -14] \% \frac{1}{s}$  in his EMS. Therefore this research uses maximal load change of  $[14.. -14] \% \frac{1}{s}$ :

$$\Delta P_{FC} \in \begin{cases} -\infty, \infty & P_{FC}(i-1) = 0 \\ 0.14, -0.14 & P_{FC}(i-1) \neq 0 \end{cases} \quad (4.14)$$

### 4.3.2. Final EMS

This will result in the final not-health aware function:

$$\begin{aligned} & \min_{u \in U} \sum_{i=1}^{i=N-1} J(x, u) \\ & J(x) = E_{H_2} = \sum_{i=0}^{i=N-1} f(P_{FC}(i)) \cdot \Delta T_i \\ \text{s.t. } & SOC \in [20, 80] \\ & \Delta P_{FC} \in \begin{cases} -\infty, \infty & P_{FC}(i-1) = 0 \\ 0.14, -0.14 & P_{FC}(i-1) \neq 0 \end{cases} \\ & P_{FC} \in [0.2, 0.8] \cdot P_{FC(\max)} \\ & \dot{SOC}_{\text{bat}}(i) = \frac{-U_0(i) + \sqrt{U_0(i)^2 - 4 \cdot P_{\text{bat}}(i) \cdot R_{\text{int}}}}{2 \cdot R_{\text{int}} \cdot C_{\text{bat}}} \\ & SOC_{\text{bat}(i+1)} = SOC(i) - \eta_{\text{bat}} \cdot \dot{SOC}_{\text{bat}}(i) \cdot \Delta T_i \end{aligned} \quad (4.15)$$

## 4.4. Health-aware EMS

According to Section 3.3.2 and Section 3.4.2 the commonly used models for degradation, are a look-up table for fuel cell degradation and an empirical model for battery degradation. If one looks at the application of these functions in literature, most papers focus on the use of an objective function where these models are used to both calculate the degradation of the components and are the objective to minimize in the cost function. Resulting in an objective function as below.

$$J(x) = \text{cost of power} \cdot \left( \frac{P}{P_{Max}} \right) + \text{cost of degradation} \cdot \left( \frac{\Delta \text{loss of Life}}{\text{Total allowable loss of Life}} \right) \quad (4.16)$$

This entails that the author of the paper determines a maximal allowable percentage of loss of life. However, as the cost of degradation is related to this percentage, the degradation part of the objective

function will have less weight at the start of the power plant lifetime and increase with the accumulated degradation/time. An example can be found using Dall'armi et al.'s [43] function:

$$\min(J(\vec{x})) = w1 \cdot f1 + w2 \cdot f2 + w3 \cdot f3 \quad (4.17)$$

where

$$f_1 = \sum_{j=1}^n \int_0^{t_{fin}} F_{FC_j} dt \quad (4.18a)$$

$$w1 = c_{H_2} = 0.3 \$ \quad (4.18b)$$

$$f_2 = \sum_{j=1}^n \int_0^{t_{fin}} dV_j(t) dt \quad (4.18c)$$

$$w2 = c_{FC} \cdot \frac{P_{FC(max)}}{V_0} \rightarrow c_{FC} = 3750 \frac{\$}{kWh} \quad (4.18d)$$

$$f_3 = \sum_{j=1}^n \int_0^{t_{fin}} Q_{loss\ battery}(t) dt \quad (4.18e)$$

$$w3 = c_{batt} \cdot \frac{E_{battery(max)}}{Q_{lossmax}} \rightarrow c_{batt} = 818 \frac{\$}{kWh} \quad (4.18f)$$

At the beginning of the lifetime, say the fuel cell operates at 50 % load and can either keep its load to charge the battery for a  $\Delta t$  or turn itself off. Also, assume that the impact of a start-stop cycle will be 1% loss of life. At  $t \approx 0$  the impact of the start-stop will be negligible (an increase from 0%  $\rightarrow$  1%), but at  $t \approx t_{final}$  this one percent increase (an increase from 90%  $\rightarrow$  91%) will have a larger weight in the overall objective function. Therefore it can be expected that for the same operation, the optimal decision will differ with time. This is also the conclusion in Dall'armi et al. [43]'s paper.

Next to the problem of the objective function not being constant over time, there is also the inaccuracy of the current degradation models as discussed in previous chapters. As stated earlier, the current degradation models are not able to capture the influence of different factors on both the battery and the fuel cell. Therefore, it is hard to quantitatively state that these models actually mitigate component degradation. And finally a fixed weight, like the cost that is given here, is not necessarily the best approach for ships, as costs of maintenance and/or components is also dependent on time-variable costs such as man-hours and knowledge in the ports that ship attains at the moment of having to replace the components (where the man-hours factor has a smaller influence in for example the price of the replacement of car components).

One can question if this is necessarily the best approach to this problem. Therefore this section will introduce a different approach to a health-aware objective function that is constant over time and calculates the response for different weights. Therefore, later in this thesis, this EMS will be benchmarked against the personal and not health-aware strategy.

#### 4.4.1. The new objectives

The objective function of this thesis differs from the literature in two ways:

- Instead of focusing on the minimization of degradation models, this objective function focuses on the actual degradation mechanisms as found in the literature.
- The objective is constant over time.
- It shows the influence of different weights for the objectives by showing the Pareto front. Based on that Pareto front actual decisions about the weights can then be made.

As stated in Section 3.2, the objective function will not minimize the models introduced in Section 3.3.2 and Section 3.4.2, but focuses instead on the actual degradation mechanisms of both the fuel cell as the battery. This section introduces the degradation mechanisms that are penalized and how they are taken into account in the objective function.

### Objective 1: fuel cell degradation

If we start by looking at the discrete degradation table (Table 3.3) of the fuel cell, four things are penalized:

1. Start-stop cycles
2. Load changes
3. High loads
4. "Idling"

From these four things, only the load changes are an actual possibility to mitigate. The mitigation of a start-stop cycle can only be achieved if future conditions are known. (For the special case of this thesis this can sometimes be true because of the dynamic approach to solving the problem). So this requires a prediction model. High and low load operations can be mitigated by constraining the operation of the fuel cell between 20% & 80% of  $P_{FCmax}$  as already done in Equation 4.11. This leaves the load changes to be mitigated. Literature also tells us that one of the causes of fuel cell degradation is fuel starvation, which according to Espiari and Aleyaasin [94]: "*Sudden load changes may result in improper water management and reactant starvation phenomena due to the slow response of the cell to load change*", which agrees with the earlier made statement. Therefore the health-aware objective for the fuel cell will become a penalty on the load changes of the fuel cell:

$$G(P_{change}, P_{FC}) = \min_{u \in \mathbb{R}} \sum_{i=0}^N \left\| \frac{P_{FC}(i) - P_{FC}(i-1)}{P_{FC}(i-1) \cdot \Delta P_{FC(max)}} \right\| \quad (4.19)$$

### Objective 2: Fuel cell efficiency

As the fuel cell is the main fuel consumer during sailing. The objective function should also contain an objective where fuel consumption is minimized. This can be done by either minimizing the total fuel consumption over time, as is done in Section 4.3, or by maximizing the total efficiency over time. But, the latter is only true for ships. Due to the nature of a power profile of a car, they should be able to turn their main power provider on or off as they will have many start and stop cycles in their power profile due to other traffic. A ship however will always have a certain base (or hotel) load and the main power-generating units will often be on when the ship is sailing, but when the ship is moored these will be turned off. Next to that, a start/stop cycle is the most impact-full degradation mechanism for the fuel cell, so we just do not give this option of starting and stopping during operation to the EMS, as the efficiency will always be zero if the fuel cell is turned off. Therefore the second objective of the total cost function will be:

$$F(\eta_{FC}, P_{FC}) = \max_{u \in \mathbb{R}} \sum_{i=0}^{N-1} \eta_{FC} = \min_{u \in \mathbb{R}} \sum_{i=0}^{N-1} -\eta_{FC} \quad (4.20)$$

### Objective 3: Battery degradation

As stated in Section 3.3.2 one of the causes of battery degradation is the formation of an SEI layer. Different papers about the causes of this SEI-layer formation are summarized in Table 4.2

**Table 4.2:** Causes SEI layer formation according to literature

Paper	Causes SEI layer formation
Edge et al. [95] Barré et al. [96] Vermeer et al. [46]	High temperature, High current. High SOC, overcharge, high temperature Furthermore, cycling, especially with high C-rates, creates a more porous SEI layer compared to idle conditions
Han et al. [97]	high SOC (lower anode potential) causing higher side reaction rates
An et al. [98]	Temperature, concentration of electrolyte salt, and reduction current rate significantly affect SEI formation as well
Edge et al. [99]	High cycling rates, high currents

The general conclusion by the papers mentioned in Table 4.2 is that the formation of the SEI layer is influenced by elevated temperature, high electric current, and high *SOC*. These factors are also reflected in Equation 3.8, except for the high *SOC*. Whilst it is challenging to account for temperature variations in this thesis due to the assumption of a constant temperature, it should be a crucial consideration in the development of an online EMS to mitigate its impact on battery performance.

Although high currents have a significant impact, Wikner and Thiringer [100] demonstrates that the *SOC* has a greater impact on battery lifespan and is thus more important to address in terms of battery life. The adverse effects of high *SOC* can be mitigated, as exemplified in Wikner and Thiringer [100]. This study shows that using a battery at a lower *SOC* range (40 – 50% instead of 80 – 90%) can double the number of cycles over the battery's lifespan. Therefore, the penalty for maintaining battery health can be expressed as follows:

$$H(\text{SOC}, P_{FC}) = \min_{u \in \mathbb{R}} \sum_{i=0}^{i=N-1} \Theta \cdot \left( \frac{\text{SOC}(i)}{M} - 1 \right) \quad (4.21)$$

where

$$\Theta = \left\{ \begin{array}{ll} 1, & \text{SOC} > M\% \\ 0, & \text{SOC} < M\% \end{array} \right\} \quad (4.22)$$

A value of 0.5 has been chosen for *M* based on the previously described doubling of battery lifespan for a *SOC* below 0.5. Additionally, this value represents a lower *SOC* that provides sufficient battery buffer, allowing the EMS to choose between using the battery or the fuel cell to meet power demand. Finally, the inclusion of  $\Theta$  in the equation ensures that the function does not encourage the utilization of the battery when the *SOC* falls below 50%. Without the inclusion of  $\Theta$ , this portion of the equation would become increasingly negative, which would promote the potentially undesired use of the battery at lower *SOC* levels.

#### 4.4.2. The health-aware cost function

Combining all the information above, we get the mathematical description of the objective function, which, combined with Figure 3.2 form the basis of the Postma health aware EMS:

$$\begin{aligned}
\min_{u \in \mathbb{R}} \varphi &= \int_{t_0}^{t_f} (J(\vec{x}, u)) dt \\
\text{s.t.} \quad J(\vec{x}, u) &= F(\eta_{FC}, P_{FC}) + G(P_{change}, P_{FC}) + H(\text{SOC}, P_{FC}) \\
F(\eta_{FC}, P_{FC}) &= \sum_{i=0}^{N-1} -\eta_{FC} \\
G(P_{change}, P_{FC}) &= w_2 \sum_{i=0}^{N-1} \left\| \frac{P_{FC}(i) - P_{FC}(i-1)}{P_{FC}(i-1) \cdot \Delta P_{FC(\max)}} \right\| \\
H(\text{SOC}, P_{FC}) &= w_3 \sum_{i=0}^{N-1} \Theta \left( \frac{\text{SOC}(i)}{0.5} - 1 \right) \\
\Theta &= \begin{cases} 1, & \text{if } \text{SOC}(i) \geq 0.5 \\ 0, & \text{if } \text{SOC}(i) < 0.5 \end{cases} \\
P_{\text{bat}}(i) &= P_{\text{req}}(i) - P_{FC}(i) \\
\dot{\text{SOC}}_{\text{bat}}(i) &= \frac{-U_0(i) + \sqrt{U_0(i)^2 - 4 \cdot P_{\text{bat}}(i) \cdot R_{\text{int}}}}{2 \cdot R_{\text{int}} \cdot C_{\text{bat}}(i)} \\
\text{SOC}_{\text{bat}(i+1)} &= \text{SOC}(i) - \eta_{\text{bat}} \cdot \dot{\text{SOC}}_{\text{bat}}(i) \cdot \Delta T_i
\end{aligned} \tag{4.23}$$

The constraints as in Equation 4.10 till Equation 4.14 still apply. As is evident from the weights, the proposed objective function exhibits a Pareto-front structure, which is in line with the previously stated notion about the weights of the objective function. Rather than solely considering component costs, as commonly seen in existing literature ([22, 28, 29, 39, 42, 43, 101, 102, 103]), the ship's owner can incorporate additional factors, such as ease of replacement and future cost predictions for the components and translate those into the 'best combination' of the weights. This distinction is particularly significant when comparing ships to cars: given that most ships have their propulsive systems in hard-to-access areas, extensive replacements or major maintenance operations will result in higher costs compared to performing similar tasks on cars. Thus, the cost function retains its relevance even if the costs of specific components fluctuate over time or the ease or difficulty of replacement actions varies.

## 4.5. EMS control strategy

Now that the EMS objective functions are known, the actual control strategy can be decided on. As the focus of this thesis is to benchmark a new 'health-aware' EMS to an EMS found in the literature, it is not necessary to use an online optimization method. As stated in Chapter 2 literature the benchmarking methods used are often based on offline solvers. Therefore, offline methods have the preference. Some of the objective functions and constraints for those functions as discussed in this chapter are non-linear, therefore a solver that can handle these non-linear functions has the preference. Finally, the method also has to guarantee that the solver can find the global minimum of the function. Jiang et al. [29] states that: '*A dynamic programming (DP) algorithm is an effective approach to solving a global optimization problem in a predefined cycle*'. As stated before, DP is often used to benchmark EMS ideas in literature, as it can guarantee the global minimum. Therefore this thesis will apply the DP method to solving this problem.

The initial paper that introduces the theory of DP is written by Bellman [104], where the following requirements are introduced

- We know all the basic variables required to describe the system.
- We are familiar with all possible decisions
- We know the general structure of cause and effect in either the deterministic or the stochastic sense
- The overall objective of the decision or control process is clearly and precisely defined.

If these requirements are met, the method or solver starts by discretizing the continuous problem. Most

simply, this means [105]:

$$x_{k+1} = F(x_k, u_k) \quad , \quad k = 0, 1, \dots, N-1 \quad (4.24)$$

where  $x$  is the state variable and  $u$  the control variable. Let  $\pi = \{u_0 \dots u_{N-1}\}$  be a control policy, and  $J$  be the total cost of that policy. The optimal control policy is:

$$J^0(x_0) = \min_{\pi \in \Pi} J_\pi(x_0) \quad (4.25)$$

This can be solved backwards by using the definition of the 'principle of optimality' according to Bellman et al. [106]: '*optimal policy has the property that whatever the initial state and initial decision are, the remaining decisions must constitute an optimal policy about the state resulting from the first decision.*'

This precise method has been rewritten into a Matlab function by Sundstrom and Guzzella [105], which is used as a benchmark in [107, 108, 109, 110, 111, 112]. Therefore, this Matlab function will be applied in this thesis.

### 4.5.1. Discrete time step

As DP is a discrete solver, time has to be discretized. This is done by splitting the problem into different time steps  $\Delta t$ . The size of each time step matters because it should be larger than the response times of the fuel cell and/or the battery, depending on which is larger.

Starting with the latter, both the fuel cell and the battery have a minimal safe response time. The time response of each component in this hybrid configuration can be found in Table 4.3. Table 4.3 shows that both the battery and the PEMFC unit can have response times in an order of up to minutes.

**Table 4.3:** Time response of different subsystems in a ship according to Bagherabadi et al. [7]

Subsystem	Time scale
Power converters switching	1 - 5 ms
Thruster drive	10 ms - 1 s
Battery charging	10 ms - 1 min
PEMFC system unit	500 ms - 1 min
Propeller inertia	1 s - 10 s

As literature (Han et al. [62], Muñoz et al. [113]) states that the PEMFC response is likely to be slower than that of the battery and that the battery can be used to deal with the transient behaviour of the PEMFC, the minimal and maximal time step are constrained by the transient behaviour of a PEMFC. According to van Biert and Visser [74] the response time of a low-temperature PEMFC is smaller or equal to 10 seconds and [114] dynamically loads a fuel cell and shows that for every cycle. That same author shows that the PEMFC manages to make a stable step of  $1.5 \text{ Acm}^{-2}$  within said ten seconds. The same author states that this step becomes unstable around 6 seconds. Therefore the discrete time step will be  $\in [6 \dots 10]$  seconds.

## 4.6. Conclusion

This chapter has introduced the mathematical foundations both for the fuel cell and battery model as well as for the three EMSs, that will be tested against each other. These EMS consist of the not-health aware EMS that only minimizes fuel consumption, the Dall'armi et al. EMS that is based on literature [43] and finally the Postma health aware EMS that both minimizes hydrogen consumption and powerplant degradation. Section 4.1 has shown a novel method of deriving the battery degradation and compared the battery model to data from the H2C boat. Section 4.3 and Section 4.4 introduced the not health aware and the previously mentioned health aware EMS's, Section 4.4 also introduced a new focus for battery degradation.

The goal is to benchmark an EMS on a known use case, a solver that can ensure the globally optimal solution for a nonlinear non-convex problem is preferred. Therefore, dynamic programming has been chosen as the method or solver to this problem. By showing the mathematical equations behind the models and the EMS's this chapter has answered sub-question 3.

# 5

## Results

The goal of this chapter is to first validate the DP model, after which the results from the multi-objective optimizations will be discussed. Before starting, it is important to establish certain KPIs for the functions in order to compare them.

As stated in previous chapters Dall'armi et al., minimizes the used degradation models and will therefore consistently outperform the personal health aware function. However, as mentioned in Chapter 4 the degradation models are not able to capture the degradation effects of all operational conditions. Therefore, the first KPI, although potentially biased, is to measure the average *SOC* of each function. This is chosen due to its previously discussed importance in battery degradation.

The second and last KPI will be the invariance in EMS behaviour over time. This KPI will indicate if there is a different bias towards objectives at the start and end of the power plant's lifetime. To measure the results of these KPIs, this chapter will first introduce a sensitivity and verification analysis of the used models. After that, it will introduce the results of the personal health aware, multi-objective EMS, after which those results are compared to the other two EMS's

### 5.1. Grid convergence study.

Before the final optimization can be started, one has to choose the discretization step of the control variable  $P_{FC}$ . This is because the amount of control choices can impact the final results. There are three objectives, all three objectives will be evaluated. The evaluation will be carried out using the not-health-aware function as that function requires the least computational power and still gives an overview of the influence of the different factors. Figure 5.1 shows the impact of the size of the array of control choices ( $Nx$ ). It shows that the fuel cell degradation, battery degradation and hydrogen consumption all converge as the number of  $Nx$  increases. Here, computational time and power start to play an important role. As the computational complexity of DP is exponential in the number of inputs and variables [105], memory usage increases fast as the amount of options increases. Due to the computational limits of the computer, the Dall'armi et al. EMS is not able to be simulated with the same amount of grid points as the Postma or not health-aware EMS. This means that the grid sizes are 25, 100,100 for the Dall'armi et al. Postma and not health-aware EMS respectively. Even though this difference might alter the eventual results, it also shows an advantage of the Postma function: due to the fewer variables that have to be carried over each time step (only the SOC and the  $P_{change}$ ), the computational complexity of this EMS is lower than the computational complexity of the Dall'armi et al. EMS.

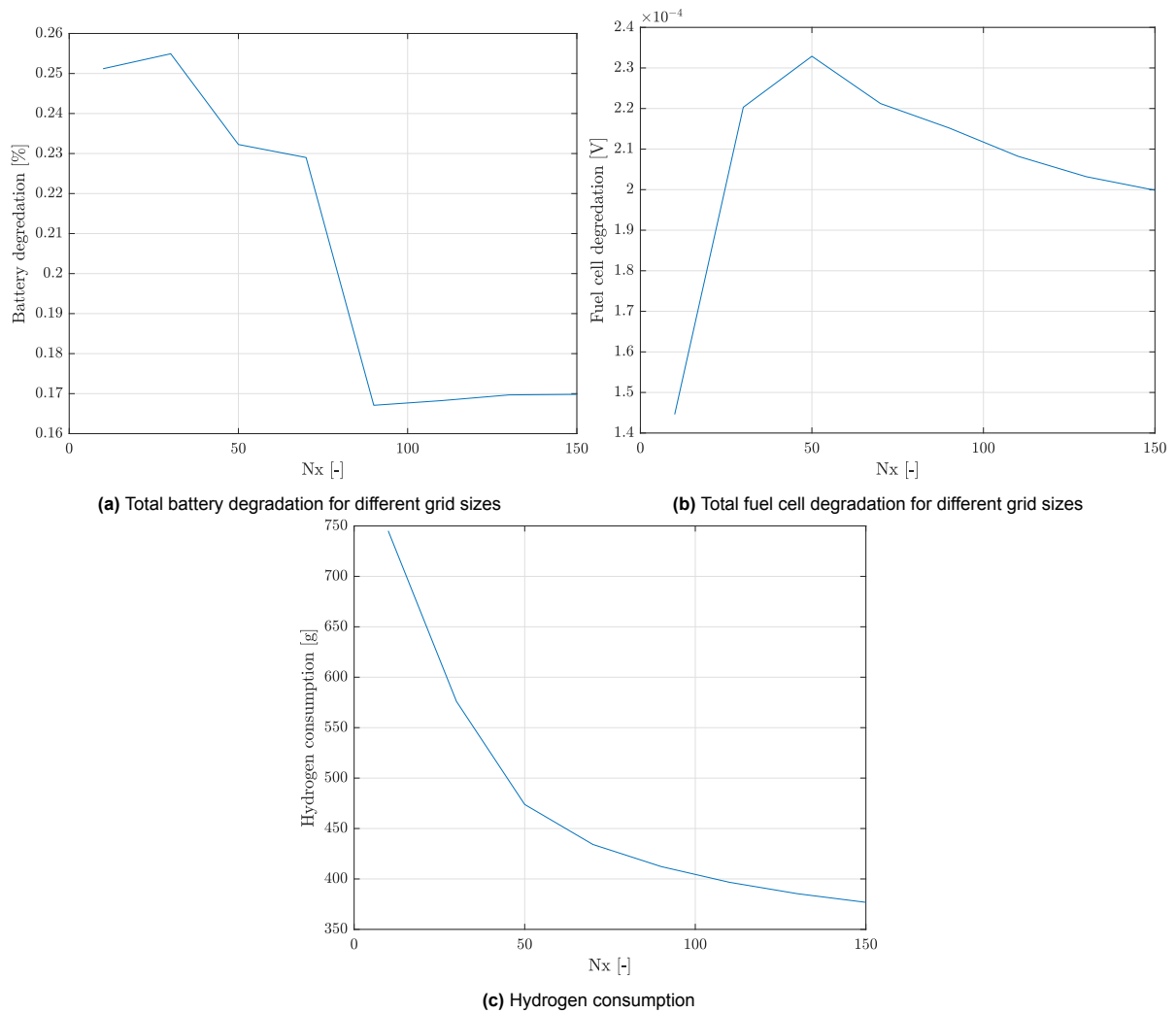


**Figure 5.1:** Grid convergence study of the battery degradation, fuel cell degradation and hydrogen consumption using the not-health aware function

## 5.2. Verification of the model

To verify that the functions and the constraints applied on the DP solver and load are viable, a verification and sensitivity analysis have been made. For these, only the not-health-aware cost function has been used, as the behaviour of that function is the easiest to predict.

Three test cases are considered:

1. Test case 1: maximize fuel consumption over a given power profile
2. Test case 2: maximize fluctuations in the behaviour of the fuel cell
3. Test case 3: Minimize fuel consumption.
4. Test case 4: Run the optimization with and without degradation.

### 5.2.1. Test case 1: maximize fuel consumption over a given power profile

In this test case, one would expect the fuel cell power to be equal to its maximum power, whenever the battery  $SOC \leq 80\%$ . Figure 5.2 shows that the fuel cell has to deliver less power at the end of the run. This is as expected, as the  $SOC$  of the battery reaches the earlier stated limit of 20%.

The maximum fuel cell power is equal to 20 kW, as already stated in the previous chapter. Figure 5.2 shows that the fuel cell operates consistently at this power, except a small part at the end of the optimization. This is caused by the battery  $SOC$  being 80 %, thus not accepting more charge from the fuel cell. It can however be concluded that the optimization works as expected.

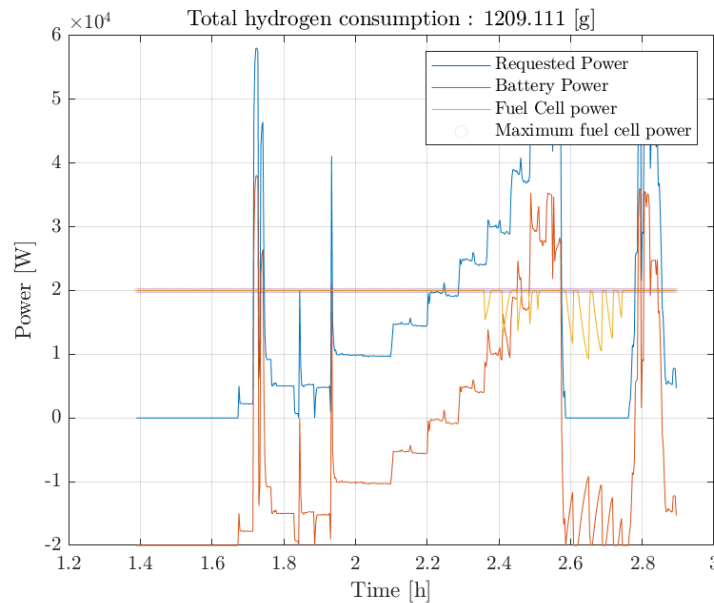


**Figure 5.2:** Results the first test case: maximize fuel consumption

### 5.2.2. Test case 2: maximize fluctuations in the behaviour of the fuel cell

In this test case, the goal is to maximize the fluctuations on the fuel cell. Therefore, one would expect the fuel cell power to fluctuate from zero to maximum power and back in each time step. If that is the case, the fluctuations are maximized over time and the DP solver does exactly what we expect it to do. Figure 5.3 shows these fluctuations over the horizon and also shows that the sum of the fuel cell and battery power is equal to the requested power. Therefore, it can be assumed that the power change is also coded correctly, which is important for both the constraints as the Postma health-aware EMS

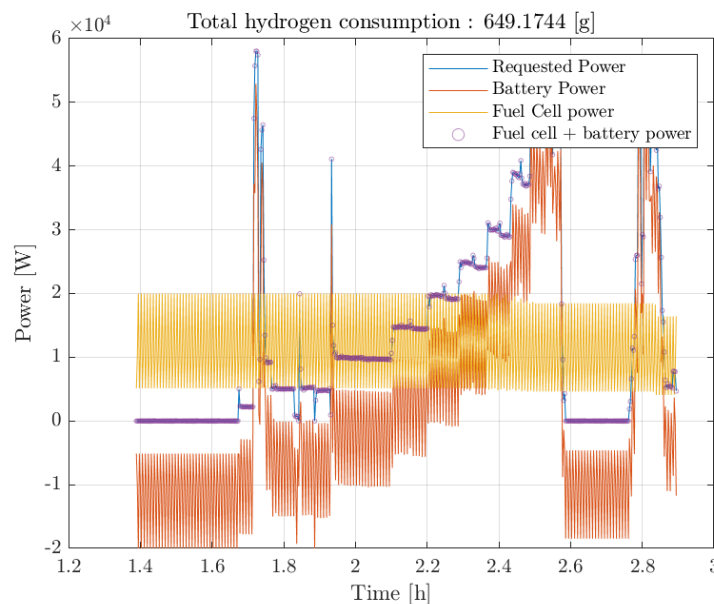


**Figure 5.3:** Results of test case 2: maximize the power changes on the fuel cell

### 5.2.3. Test case 3: Minimize fuel consumption

Test case 3 shows that the optimization can also be used to minimize parameters. In this test case, the hydrogen consumption of the fuel cell is minimized, resulting in Figure 5.4. Figure 5.4 shows that

fuel consumption can be minimized. Sundstrom and Guzzella [105] shows that the DP function can find the global minimum, therefore we can assume that the found minimum is also the global minimum solution.

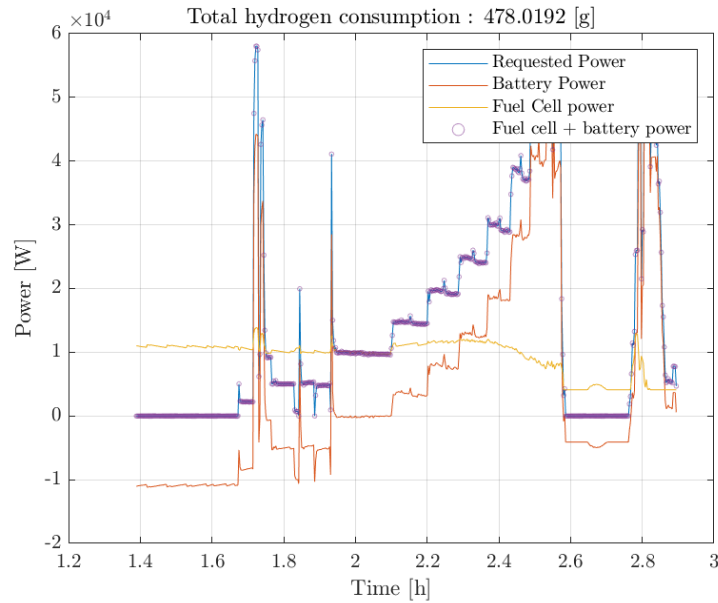


**Figure 5.4:** Results of test case 3: minimize hydrogen consumption

#### 5.2.4. Test case 4: Run the optimization with and without degradation

Even though test case 4 is a bit different from the other test cases, the important factor here is to see if the degradation changes the behaviour of the system. One would expect a system with lost capacity to be less efficient and consume more hydrogen over time. Figure 5.5 shows the optimal hydrogen consumption results from the optimization over time. It follows the idea introduced in chapter 3, so it optimizes one run and runs those results for two weeks, 5 times a day and then goes to the next 'optimization'. It can be concluded that hydrogen consumption increases over time if degradation is taken into account. Where degradation is not taken into account, the hydrogen consumption of the optimization is constant.

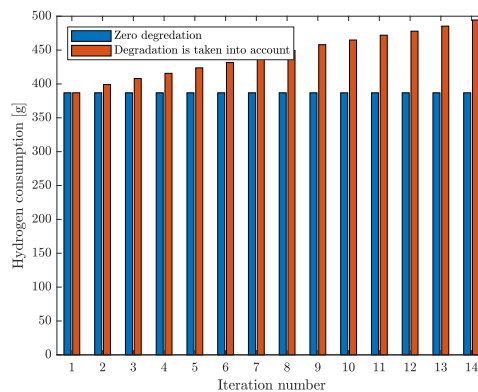


**Figure 5.5:** Results of test case 4: Run the optimization with and without degradation.

If we look at the results of the four test cases, it can be concluded that the solver and model respond as can be expected. Therefore, we can continue and compare the results of the different optimizations.

### 5.3. Multi-objective optimization results.

In this section, the results of the multi-objective optimization will be discussed. Figure 5.6 shows the point-cloud generated by alternating the weights ( $\lambda_1$  &  $\lambda_2$ ). Different perspectives of this point cloud containing the Pareto-fronts can be found in Appendix A. With the use of costs for the different objectives as found in literature, two optimal weights ( $\lambda_1$  &  $\lambda_2$ ) will be chosen to compare the results to the not-health aware benchmark and the Dall'armi et al. health aware optimization. To also give an overview of the effects of ( $\lambda_1$  &  $\lambda_2$ ) on the different objectives, the results are interpolated and plotted in the coming sections.

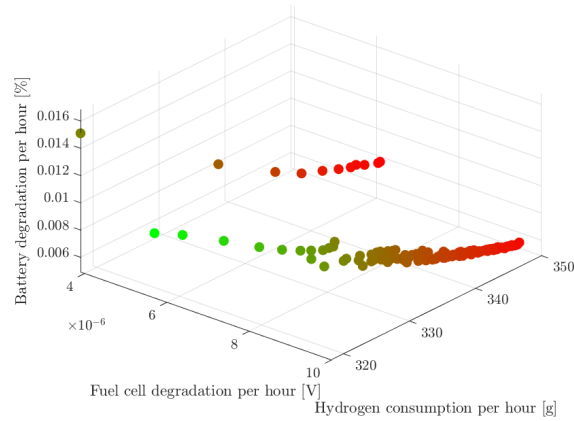


Figure 5.6: Generated Pareto front

#### 5.3.1. Effect on fuel consumption

Figure 5.7 shows that  $\lambda_2$  has a high influence on the fuel cell fuel consumption. This is likely caused by the fact that the third objective promotes a low battery *SOC*. If we were to look at the power distribution of the optimization where  $\lambda_2$  is 0, or 1 (whilst  $\lambda_1 = 0$ ), as done in Figure 5.8, we can see that if  $\lambda_2 = 0$  the battery charges in the initial phase, resulting in having to operate at a lower power further on. The graph of  $\lambda_2 = 1$  shows that initially, the battery is not charged (as the objective function aims for a lower *SOC*). This directly entails that later on the fuel cell has to deliver more power. At this point, the fuel cell operates at lower efficiency, thus even if the total delivered power from both graphs is equal, the hydrogen consumption for the  $\lambda_2 = 1$  is higher.

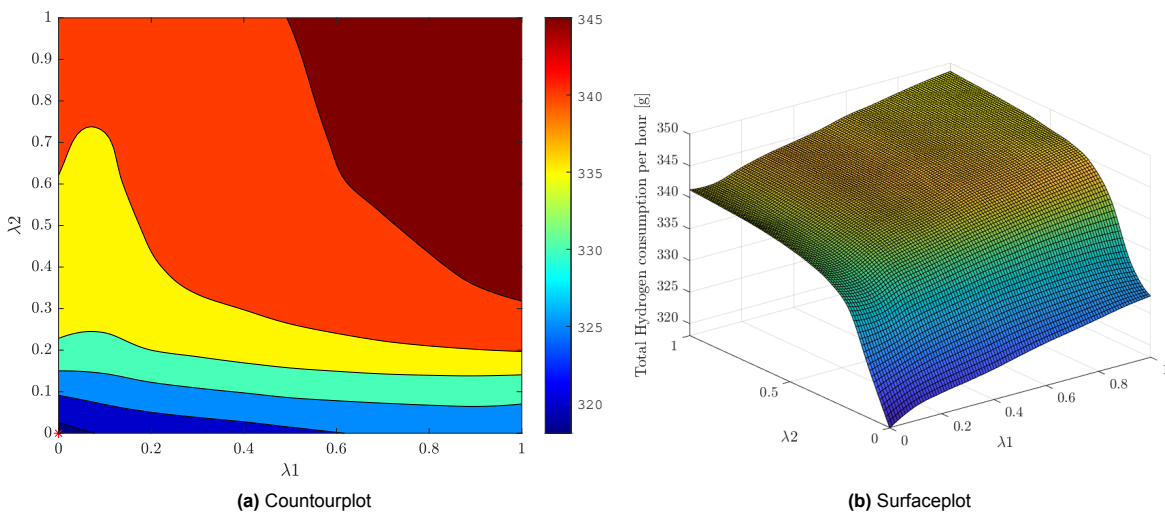
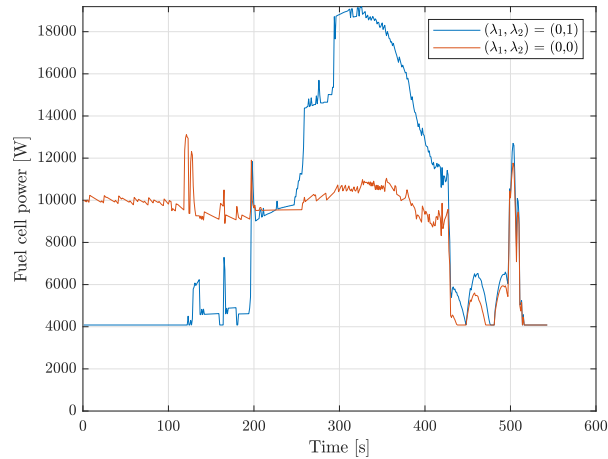


Figure 5.7: Results of the hydrogen consumption per hour coming from the Postma health aware EMS



**Figure 5.8:** Differences in optimal power distribution between for the first optimization step of different  $\lambda_2$ 's

### 5.3.2. Effect on fuel cell degradation

Figure 5.9 shows the degradation of the fuel cell for different weights. due to the relatively zero gradient in the x-direction, it becomes clear that the influence of  $\lambda_1$  has little influence on the overall fuel cell degradation. This can be explained by the fact that the weight of  $\lambda_1$  is given to the part of the objective function that penalizes the power changes. However, the objective function also tries to maximize the efficiency of the fuel cell. As the point of maximum efficiency does not change during one iteration, the power fluctuations are already brought to a minimum as it aims to operate at that point most of the time. The  $\lambda_2$  does have a significant impact, which can be explained using Figure 5.8. In Figure 5.8 it is clear that a larger  $\lambda_2$  results in larger fluctuations in the power of the fuel cell, thus resulting in more degradation.

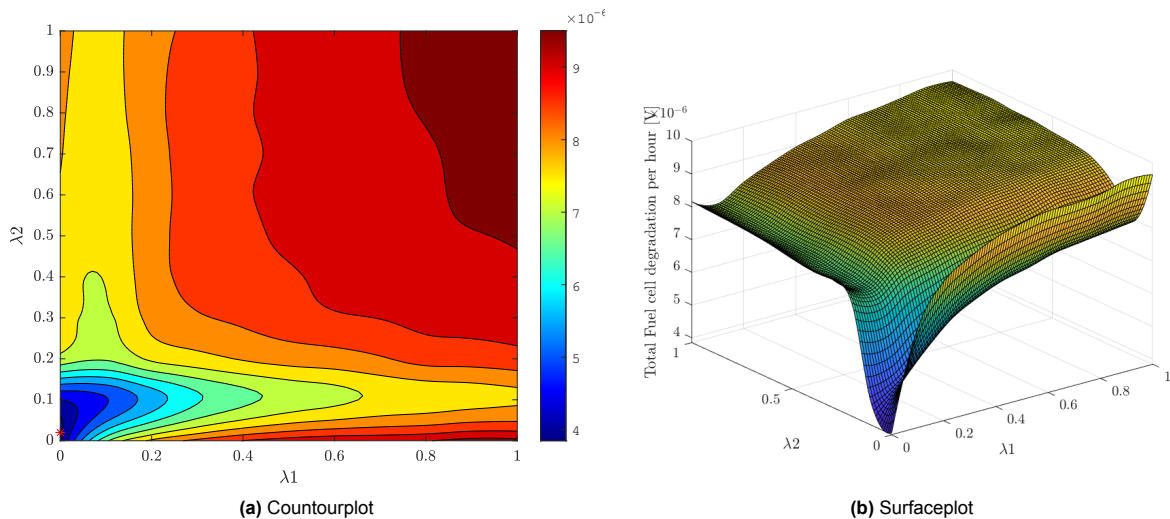


**Figure 5.9:** Results of the fuel cell degradation per hour resulting from the Postma health aware EMS

### 5.3.3. Effect on battery degradation

The final objective to discuss is the battery degradation and the effect of the different  $\lambda$ 's. As the degradation model does not consider the battery *SOC* as a degradation parameter, it is interesting to see that aiming for a lower *SOC* still has a positive effect on the battery degradation. This is most likely caused by the lower charges that are put through the battery during the optimal power distribution.

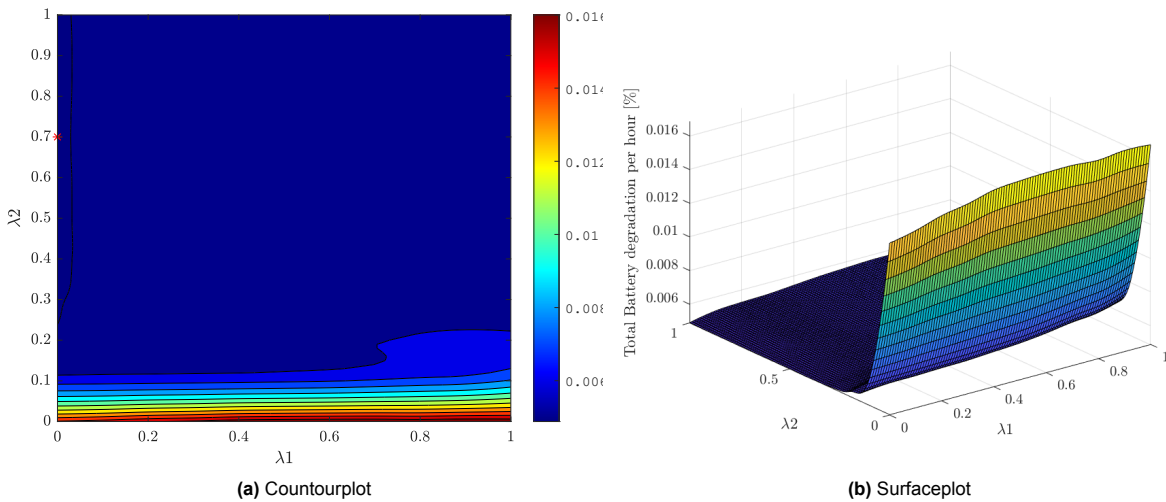


Figure 5.10: Results of the battery degradation per hour resulting from the Postma health aware EMS

### 5.3.4. Equivalent costs

To see the combined effect of the total power plant, the OPEX is considered for the calculations. The degradation of the fuel cell and the battery are part of these OPEX in the form of a reservation. So, how much money does the owner have to save to be able to buy a new fuel cell or/and battery when the current fuel cell/battery is written off? As this is only part of the thesis, it is important to note that no installation costs have been taken into account for this calculation. However, as stated before, especially for ships, this might be an important factor for later calculations/determination of the weights. To do this, the costs of hydrogen, a LT-PEMFC and a Li-ion battery have to be researched using literature.

#### Cost of hydrogen

According to the research conducted by Ajanovic et al. [5], the cost of green hydrogen, which serves as the benchmark in this context, is reported to range from 2.2 to 8.3 euro per kilogram at the time of writing his paper. For this thesis, the maximal cost of green hydrogen will be taken as the important parameter. Therefore, the cost of hydrogen will be equal to 8.3 dollars per kilogram (the dollar is about equal to the euro at the moment of writing).

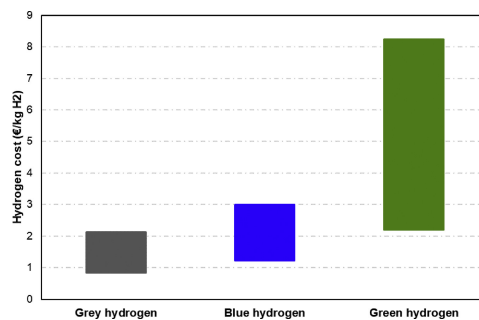


Figure 5.11: Cost of hydrogen according to Ajanovic et al. [5]

#### Capital cost of the LT-PEMFC

According to van Biert and Visser [74], the capital cost of a PEMFC in 2030 is between 60 and 600 \$/kW. Wang et al. [16] states that the fuel cell propulsion system of the fuel cell hybrid vehicle proposed in that paper will cost about 180 dollars per kW. However, these costs are for a car, not a ship. Therefore, this thesis will take the costs right in between the costs stated in [16] and [74]; a cost of 400 \$ per kW.

#### Capital costs of the Li-ion Battery

According to Ding et al. [115] 'the capital costs are on a trajectory toward about 340 \$/kWh for installed stationary systems'. Feldman et al. [116] states that the costs of batteries are equal to \$341/kWh.

These costs are expected to drop by approximately 20 % in 2030 if one would look at the high margin found in Cole et al. [117]. As this prediction from Cole et al. contains a high uncertainty (the low limit is equal to 80 %) this thesis uses 80 % of 340 \$/kWh as a cost for the battery system.

### Combined results

Figure 5.12 shows the results of the combined costs. The absolute minimal cost is indicated with a red star. The figure shows that the lowest cost can be found in the region where  $\lambda_1$  is equal to zero and  $\lambda_2$  is equal to 0.7. Figure 5.12 also shows that the influence of  $\lambda_1$  is relatively low, and only a difference in  $\lambda_2$  results in truly lower costs.

One can also clearly see that by lowering the second weight, the cost increases. This is mostly caused by the decrease in overall power plant lifetime and therefore an increase in daily operating costs. In this case, that would mean that the weights of this result will be used to quantitatively compare the 3 different EMSs.

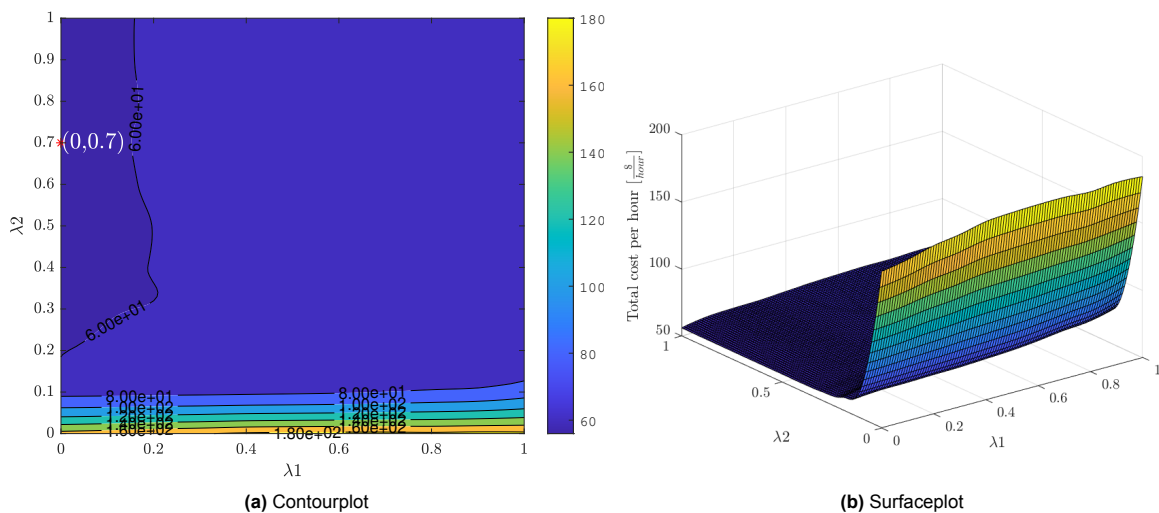


**Figure 5.12:** Hourly operating costs of the entire system using the Postma health aware function

## 5.4. Comparison between 3 EMS

This section compares the overall results. It will start by showing the results for the hydrogen consumption, fuel cell degradation and battery degradation. After which, each objective will be discussed individually in more detail. The end of this section focuses on the potential profit of the health-aware functions.

### 5.4.1. Results for all three objectives

Figure 5.13 shows the comparison between the health-aware function as discussed in Dall'armi et al. [43], the not health-aware function as discussed in Section 4.3 and finally the health-aware function as discussed in Section 4.4. One can see that (as expected) the Dall'armi et al. EMS manages to survive the longest. This is likely due to the minimization of the degradation functions. One can also see a large difference in fuel cell hydrogen consumption per iteration (Figure 5.13c). Even though the Dall'armi et al. EMS will have a larger hydrogen consumption than the other EMSs, the difference is also enlarged due to the smaller grid size. It can be expected that the fuel cell hydrogen consumption, in reality, is about 200-300 grams lower than what is shown in this graph.

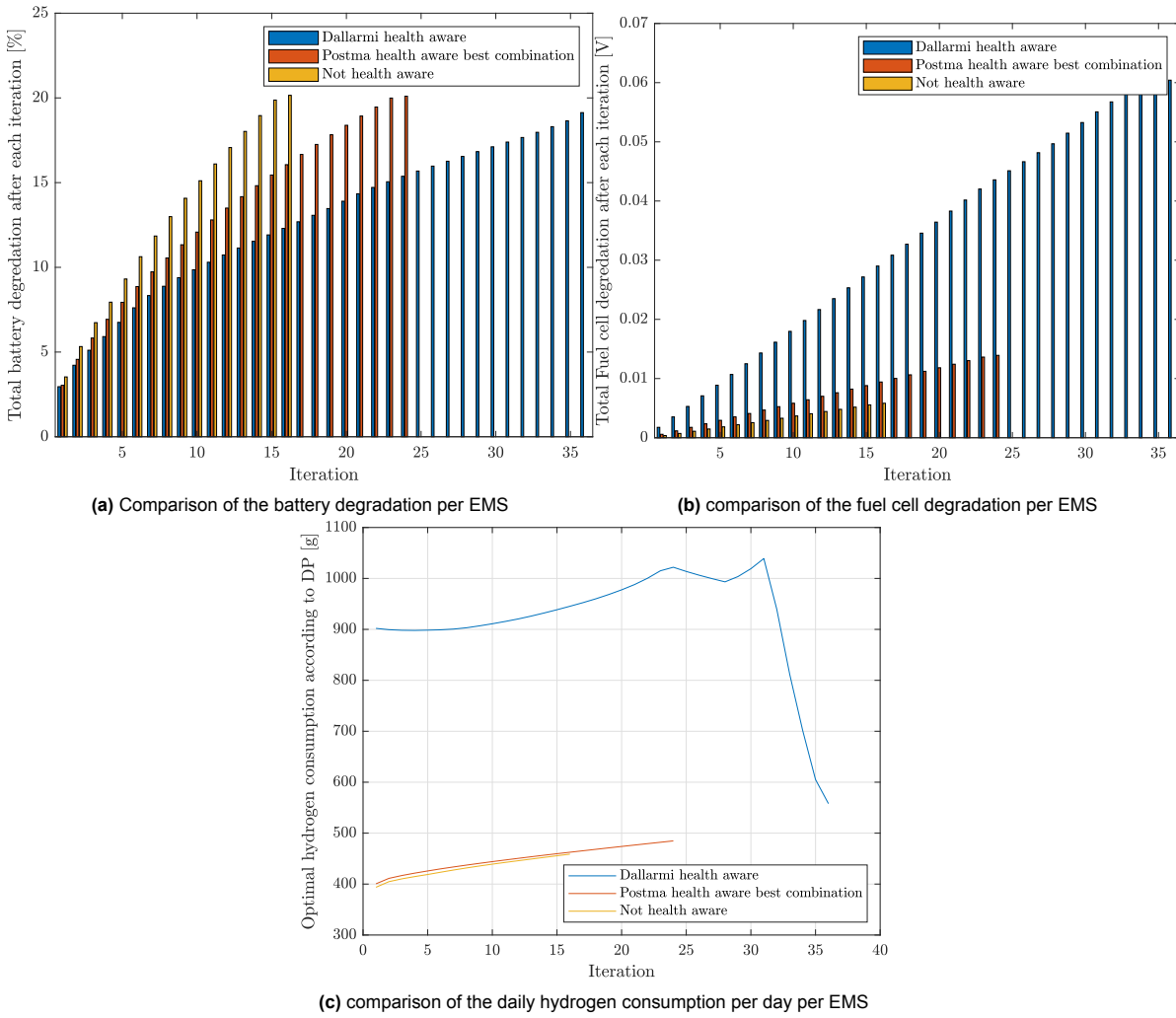


**Figure 5.13:** Comparison of the resulting battery degradation, fuel cell degradation and hydrogen consumption of each EMS

### 5.4.2. Power distributions of each run

Figure 5.13 can be explained by how the EMS decides to distribute power between the different components. As the decision process of every optimization is hard to visualise, this has been done by gathering the range of values of the power  $P_{FC}$  for each time step  $\Delta t$  and plotting the maximum, minimum and average power choice, this results in Figure 5.14. Figure 5.14 shows a couple of interesting things, starting with the fact that Postma EMS power distribution chooses to not charge the battery at the beginning of the requested power cycle. There where both the not health-aware and the Dall’armi et al. health-aware function do choose to charge the battery, most likely because the two latter functions minimize hydrogen consumption, whilst the Postma health-aware function does not do so.

Figure 5.14 also shows how the different functions respond to the degradation of the components. There were the not health-aware and Dall’armi et al. both respond to degradation by changing their decisions across the entire time domain, the Postma health-aware only makes changes after about 2500 seconds. This can again be related to the decision of keeping the SOC of the battery low, as this is the first point in the requested power graph where the requested power is above the maximum deliverable power from the fuel cell ( $2 \cdot 10^4 W$ ). Finally Figure 5.14 also confirms that the Dall’armi et al. will have a higher hydrogen consumption, as the average power is higher than for the other two EMS. This average is somewhat dependent on the grid size, however, the differences are so large that one can safely state that the Dall’armi et al. EMS will have a larger difference in hydrogen consumption.

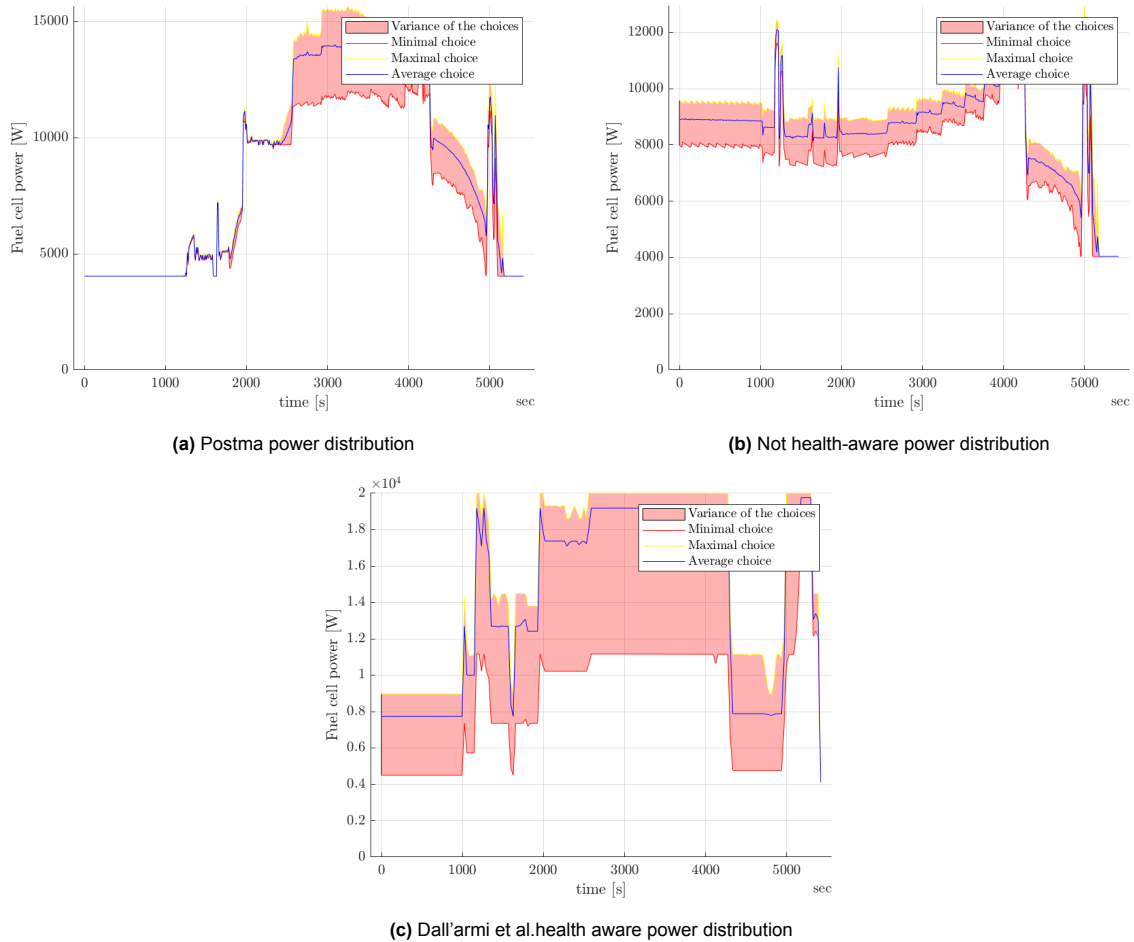


**Figure 5.14:** Comparison of the power distributions of the different EMS

### 5.4.3. Effect on fuel cell degradation

Figure 5.13b showed that the not health-aware function has the least fuel cell degradation. This is most likely due to the relatively constant power that is asked from the fuel cell by the EMS. All distributions go through the same start/stop cycle, as none of them turn off the fuel cell during operation. Therefore, the biggest factor influencing fuel cell degradation is power change. As can be seen in Figure 5.14, the not health-aware function has the least relative power change over the runs compared to the other two functions, therefore resulting in a lower degradation.

### 5.4.4. Effects on Battery degradation

This subsection elaborates on the effects of the battery degradation. What is interesting here, is not necessarily the accumulated degradation, but more the effects on the *SOC*. As the distribution of the *SOC* shows if the Postma health-aware function worked, or whether the penalty on the *SOC* does not affect the battery load. Figure 5.15 clearly shows that the distribution of the *SOC* over the power plant lifetime lies lower than the distribution of the not health aware, resulting in the conclusion that the penalty on the *SOC* does impact results.

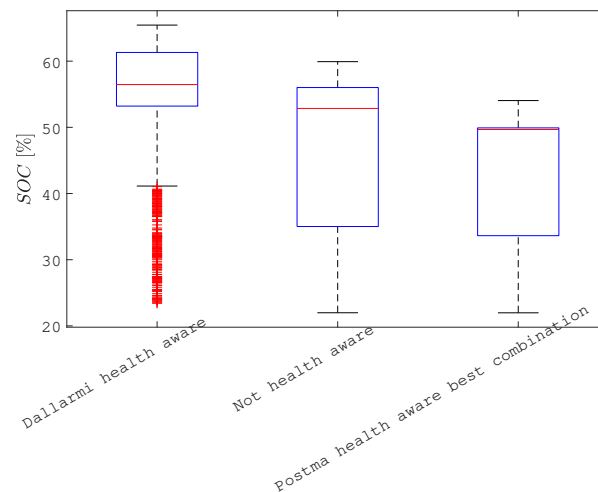


**Figure 5.15:** Resulting *SOC* distribution of each EMS

#### 5.4.5. Comparison of the daily operating costs.

This sub-section aims to compare the different outcomes of the optimizations. Table 5.1 shows different other Key performance indicators (KPI) about the EMS performance. What becomes clear, is that the Dall'armi et al.'s EMS manages to outperform each of the other EMSs, especially on the average daily operating costs. This is in line with what one would expect, because even though the costs of each objective are different from the costs used in this thesis, in essence, Dall'armi et al. still minimizes the average daily operating costs, whilst the Postma health aware function does not optimise for these costs.

**Table 5.1:** Costs per day.

	<b>Not health aware</b>	<b>Postma health aware</b>	<b>Dallarmi health aware</b>
Total Powerplant lifetime [h]	1.686E+03	33%	56%
Average battery degradation per day	8.997E-02	-50%	-137%
Average fuel cell degradation per day	2.600E-05	37%	78%
Average hydrogen consumption per day	2.157E+03	4%	53%
<b>Average daily operating costs</b>	<b>\$ 996.81</b>	<b>-49%</b>	<b>-121%</b>

## 5.5. Conclusion

The goal of this section was to verify the models that were built and then elaborate on the results of the optimization. As shown in Section 5.2 the DP optimization works as expected. To compare the results, the introduction of this chapter introduced two KPIs:

- The height of the average *SOC*.
- The variance of the EMS function over time.

*KPI 1: Height of the average SOC:* Figure 5.15 clearly shows that the average *SOC* of the personal health aware function is lower than that of both of the other functions. This is mostly due to the different nature of the three functions, as the personal health aware function is the only function that actually penalizes this high *SOC*. However, it does mean that, if we follow the earlier statement about this *SOC*, that the personal health aware EMS outperforms the other two.

*KPI 2: Little invariance in the bias of the EMS function over time:* Figure 5.14 shows that the personal health aware function does not really differ its strategy over time, it just changes in accordance with the degradation. The not health aware function also follows this trend, as apparently even after degradation the initial optimization still delivers the least hydrogen consumption. Dall'armi et al.'s function, however, does show changes over time. This was to be expected because of the nature of the function, where the weights of each objective change over time.

If we look at these KPIs, the personal health aware function demonstrates better Energy Management System (EMS) performance compared to the other two functions. However, it is important to acknowledge significant limitations in this statement. Section 5.4.5 shows that if the KPIs were different, say for example powerplant lifetime or daily operating costs, the outcome would have been different.

# 6

## Discussion

The goal of this thesis is to answer the main research question:

*'What is the impact of including component degradation in advanced energy management strategies on energy consumption and power plant lifetime for fuel cell-battery powered vessels?'*

The short answer to this question is that the impact on the components is measurable and can therefore be used in both the EMS and the actual models of each component. However, the discussed models are subjected to multiple limitations:

- According to Vermeer et al. [46] the battery degradation model only takes early aging into account. After about 3000 *Ahr* different effects start to play a role in the battery degradation.
- There is no validation of the battery degradation function to see the effects of different (dis)-charging cycles, therefore one can question the validity of the empirical model for describing degradation of multiple stacked cycles.
- Even though not all batteries and fuel cells are created equal, the degradation models used to describe degradation behaviour are standardized in literature. On top of that, the formula that is used dates from 2011. In the mean time batteries have made major improvements, therefore likely resulting in different degradation behaviour.
- No validation or verification possible of the fuel cell degradation model.
- Only limited information available about the fuel cell.
- Unsure about validity of the programming of Dall'armi et al.'s function.
- Both the battery and fuel cell model are heavily simplified to aid in simpler calculations.
- Section 5.1 has shown that the size of the grid has a large influence on all three objectives that are measured in the results. Therefore, for example, the daily operating costs of the Dall'armi et al. EMS could be even lower.

If one combines these statements, a righteous question that can be asked is if the results are reliable. If one were to look at literature, different papers show their results without comparing them with the influence of the errors of their models, even though the accuracy of these models can have a large influence on the actual results.

However, the problem is even larger, as the results are always measured against author defined KPI's. By measuring the results against these author defined KPI's, one will inherently get subjective results, as no author will measure against KPI's where his or her EMS performs worse.

But, showing that the Postma health aware EMS outperforms every other EMS was not the goal of this research. The goal of this thesis was to show the impact of including component degradation, whilst using diagnostic tactics in the EMS. Where literature aims to minimize degradation models that are shown to not always guarantee accurate results. If we were to look at Chapter 5, this goal has been reached, as the results show that the EMS is both aware of it's impact on the powerplant as takes the degradation caused on the powerplant into account.

Finally, it is also interesting to discuss the influence of the factor  $M$  in the Postma-health aware function as described in Equation 4.23, as that will inevitably alter the results. To do this, the weights

as chosen in section 5.3 are used whilst  $M$  was altered between zero and one, resulting in the  $SOC$  distribution as can be found in Figure 6.1

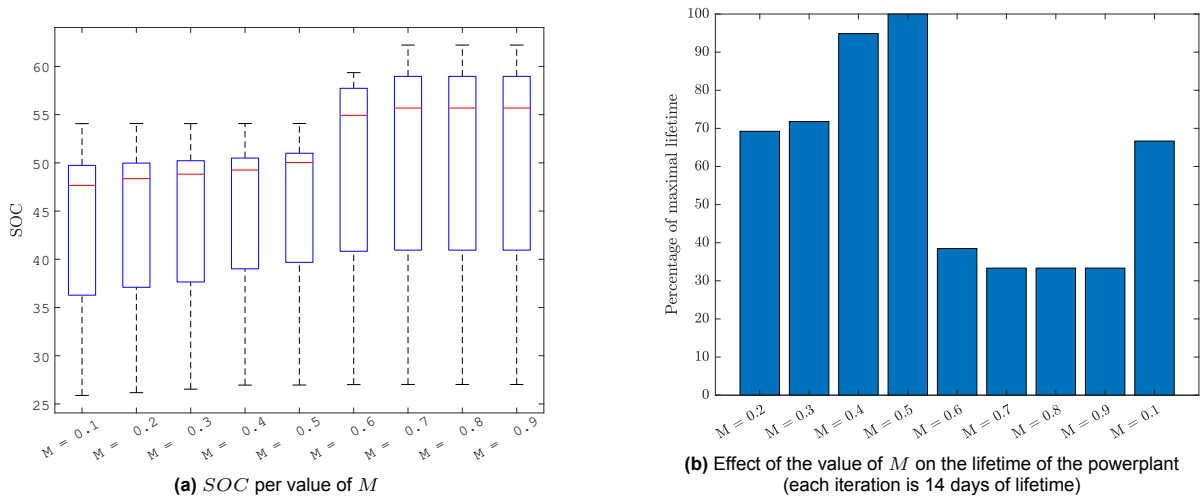


Figure 6.1: Effects of changing the value of  $M$

The threshold of 0.5 is a dividing line between two optimization approaches, evident from Figure 6.1a. For values of  $M < 0.5$ , the EMS prioritizes minimal initial battery charging, resulting in increased fuel cell workload later on, but an overall lower  $SOC$  of the battery. Conversely, above 0.5, the EMS opts for early battery charging. This disparity can be attributed to the battery's considerable size, wherein the SOC typically reaches a maximum of 0.67, allowing sustained fuel cell power output. Notably, the EMS with a 0.5 threshold exhibits the longest lifespan, as depicted in Figure 6.1b. This is likely due to lower penalties ( $<0.5$ ) causing smaller power fluctuations and thus decreased degradation for both the battery and fuel cell. Above 0.5, the power choices of the optimization start to align with the non-health-aware EMS, yielding the power distribution as discussed in section 5.4. In conclusion, the significant impact of the penalty value ( $M$ ) on the system is noteworthy, but the choice of 0.5 seems to be the optimal value for this problem.

Sticking with the degradation penalty used for the battery, earlier in the thesis it was stated that for online methods, it might be better to penalize high battery temperatures, as most (or all) literature seems to agree that temperatures have the biggest effect on the degradation of batteries. For example, Figure 6.2 shows us how large of an effect this temperature can have. Therefore, future online research should focus on penalizing battery temperature instead of penalizing the battery  $SOC$

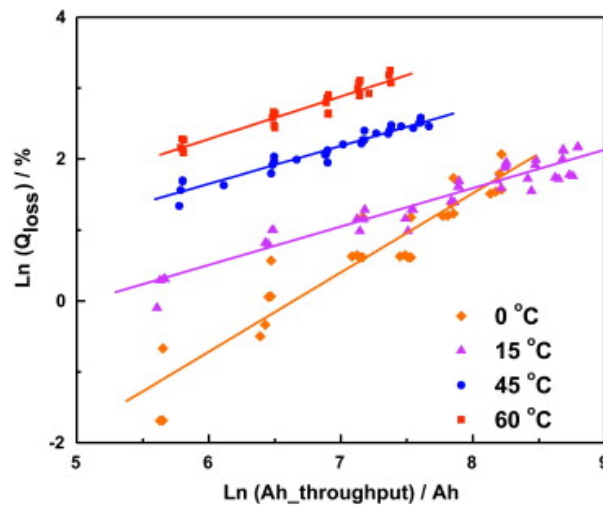


Figure 6.2: Relation between temperature and battery degradation according to Wang et al. [6]

To conclude the discussion, by combining the statement of the KPIs and the model limitations, one can state that at this moment much is unclear about the actual degradation behaviour of batteries and fuel cells in different operating conditions. Therefore the step towards online health aware energy management systems (as the literature has not seen any online test cases) needs a different way of looking towards this problem. Instead of asking the question: 'What is the impact of degradation', the energy management question should be more about 'What can an EMS do to mitigate the causes of this degradation'. So instead of trying to measure the impact, it should aim to penalize certain actions. This also allows for uncertainty in the operational future as the penalty will be constant over time. To be able to do this, more research on component degradation is needed. As that will allow us to both better understand the degrading mechanisms of components, and also enables us to make better state estimations based on data from those components. This thesis shows that this diagnostic approach to making systems health aware can work, but to effectively see the effects of this way of thinking, it should be tested in an online environment.



# 7

## Conclusion

In the introduction of this thesis, three sub-questions have been introduced. The conclusion will first answer these sub-questions, after which the answer to the main research question of this thesis will be discussed.

Regarding the state-of-the-art in health aware energy management systems, Chapter 2 reviewed existing literature and identified a gap in diagnostic health aware systems. It was found that the degradation models that are most often used may not fully capture the behaviour of batteries or fuel cells under most operating conditions. As most prognostic health aware systems seem to aim to minimize these models in their objective functions, this research focused on a diagnostic approach that aims to minimize causes for degradation instead of questionable degradation models.

Chapter 3 introduced the test case (the H<sub>2</sub>C boat [47]) and the methodology behind the virtual power plant and the energy management system, and explained the different causes of degradation for both the battery cell and the low-temperature PEM fuel cell, plus models that describe this degradation behaviour. By doing so, it answered sub-question two. The conclusion of this chapter formed the foundation for the actual mathematical model that has been developed in Chapter 4 consisted of computationally not too complex models that were still able to describe power plant behaviour, subject to some assumptions. It also showed that while the EMS-model layout remained the same for the not-health-aware and personal health aware EMS, the cost functions differed.

In Chapter 4 the mathematical foundations of the virtual models were presented. This showed the necessity for a different manner of discretizing the mathematical model that describes the degradation of the battery. After the virtual models of the battery and the fuel cell were introduced, the mathematical foundations for the three EMS objective functions were introduced. The not health aware EMS aimed to purely minimize hydrogen consumption. The EMS from the literature was based on the objective function found in Dall'armi et al. [43]. Finally, the EMS that was developed in this thesis was introduced. This EMS aims to maximize fuel cell efficiency, minimize power fluctuations, and penalize high battery *SOC*. The EMS objectives aimed to minimize power plant component degradation and reduce fuel consumption. Finally, this chapter also introduced the method (dynamic programming) that was used to solve the objective functions.

In Chapter 5 a sensitivity analysis, validation of the models and the results were presented. It showed the sensitivity of the model for changes in the grid size, and that the model behaved as expected. It showed that by maximizing fuel cell efficiency, the personal health aware EMS also minimized power fluctuations and thus the second objective remained without function and can be discarded. Furthermore, it showed that the Postma health-aware EMS outperformed the other functions based on different KPIs. However, objectively measuring this impact is challenging due to the subjective nature of KPIs and uncertainties in future component costs and degradation models. For example, the Dall'armi et al. EMS outperformed the other functions based on a daily operating cost estimation.

To answer the main research question:

*'What is the impact of including component degradation in advanced energy management strategies on energy consumption and power plant lifetime for fuel cell-battery powered vessels?'*

Taking health into account does have an impact on the performance of the EMS and the power plant. However, objectively measuring this impact is challenging due to the subjective nature of KPIs and uncertainties in future component costs and degradation models.

Consequently, this research concludes that further investigation is necessary for component degradation. This would enable improved models capable of estimating the current component health based on various parameters. Additionally, it would empower EMSs to better comprehend the impact of their operations by penalizing specific operating conditions that are known to have a substantial negative effect on the lifespan of the power plant.

In summary, this research contributes to the understanding of the impact of health aware energy management systems. Instead of the popular prognostic approach, this thesis aimed at using a diagnostic approach whilst also suggesting known and new mathematical models for powerplant components in a fuel cell and battery hybrid ship. Conclusively, it suggests avenues for future investigation. By following these avenues, the development of more effective and unbiased health-aware EMS's can be realized.

# Bibliography

- [1] inci Mustafa, Büyük Mehmet, Hakan Demir Mehmet, and ilbey Göktürk. A review and research on fuel cell electric vehicles: Topologies, power electronic converters, energy management methods, technical challenges, marketing and future aspects. *Renewable and Sustainable Energy Reviews*, 137:110648, 3 2021. ISSN 1364-0321. doi: 10.1016/J.RSER.2020.110648.
- [2] Nikolaos Planakis, George Papalambrou, and Nikolaos Kyrtatos. Ship energy management system development and experimental evaluation utilizing marine loading cycles based on machine learning techniques. *Applied Energy*, 307:118085, 2 2022. ISSN 0306-2619. doi: 10.1016/J.APENERGY.2021.118085.
- [3] A J Appleby and F.R. Foulkes. *Fuel cell handbook*. U.S. Department of Energy, 1 1988. URL <https://www.osti.gov/biblio/5616450>.
- [4] Dawn Mcintosh. Li-ion battery aging datasets | nasa open data portal, 2019 (accessed 25-01-2022). URL <https://data.nasa.gov/dataset/Li-ion-Battery-Aging-Datasets/uj5r-zjdb>.
- [5] A. Ajanovic, M. Sayer, and R. Haas. The economics and the environmental benignity of different colors of hydrogen. *International Journal of Hydrogen Energy*, 47(57):24136–24154, 2022. ISSN 0360-3199. doi: <https://doi.org/10.1016/j.ijhydene.2022.02.094>. URL <https://www.sciencedirect.com/science/article/pii/S0360319922007066>. Hydrogen Society.
- [6] John Wang, Ping Liu, Jocelyn Hicks-Garner, Elena Sherman, Souren Soukiazian, Mark Verbrugge, Harshad Tataria, James Musser, and Peter Finamore. Cycle-life model for graphite-LiFePO4 cells. *Journal of Power Sources*, 196(8):3942–3948, 4 2011. ISSN 0378-7753. doi: 10.1016/J.JPOWSOUR.2010.11.134.
- [7] Kamyar Maleki Bagherabadi, Stian Skjong, Jogchum Bruinsma, and Eilif Pedersen. System-level modeling of marine power plant with pemfc system and battery. *International Journal of Naval Architecture and Ocean Engineering*, 14:100487, 2022. ISSN 2092-6782. doi: <https://doi.org/10.1016/j.ijnaoe.2022.100487>. URL <https://www.sciencedirect.com/science/article/pii/S209267822200053X>.
- [8] IMO. Fourth imo ghg study 2020 full report: Tech. rep., 2020, (accessed 11-12-2022). URL <https://www.imo.org/en/OurWork/Environment/Pages/Fourth-IMO-Greenhouse-Gas-Study-2020.aspx>.
- [9] R. D. Geertsma, R. R. Negenborn, K. Visser, and J. J. Hopman. Design and control of hybrid power and propulsion systems for smart ships: A review of developments. *Applied Energy*, 194: 30–54, 2017. ISSN 03062619. doi: 10.1016/J.APENERGY.2017.02.060.
- [10] Asgeir J. Sorensen, Roger Skjetne, Torstein Bo, Michel R. Miyazaki, Tor Arne Johansen, Ingrid B. Utne, and Eilif Pedersen. Toward Safer, Smarter, and Greener Ships: Using Hybrid Marine Power Plants. *IEEE Electrification Magazine*, 5(3):68–73, 9 2017. ISSN 2325-5897. doi: 10.1109/MELE.2017.2718861.
- [11] Hoang Phuong Nguyen, Anh Tuan Hoang, Sandro Nizetic, Xuan Phuong Nguyen, Anh Tuan Le, Cong Nho Luong, Van Dat Chu, and Van Viet Pham. The electric propulsion system as a green solution for management strategy of CO2 emission in ocean shipping: A comprehensive review. *International Transactions on Electrical Energy Systems*, 31(11), 11 2021. ISSN 20507038. doi: 10.1002/2050-7038.12580.
- [12] Omer Berkehan Inal, Jean Frédéric Charpentier, and Cengiz Deniz. Hybrid power and propulsion systems for ships: Current status and future challenges. *Renewable and Sustainable Energy Reviews*, 156:111965, 3 2022. ISSN 1364-0321. doi: 10.1016/J.RSER.2021.111965.

- [13] Jens F. Peters, Manuel Baumann, Benedikt Zimmermann, Jessica Braun, and Marcel Weil. The environmental impact of Li-Ion batteries and the role of key parameters – A review. *Renewable and Sustainable Energy Reviews*, 67:491–506, 1 2017. ISSN 1364-0321. doi: 10.1016/J.RSER.2016.08.039.
- [14] L. van Biert, M. Godjevac, K. Visser, and P. V. Aravind. A review of fuel cell systems for maritime applications. *Journal of Power Sources*, 327:345–364, 9 2016. ISSN 0378-7753. doi: 10.1016/J.JPOWSOUR.2016.07.007.
- [15] M. Kandidayeni, J. P. Trovão, M. Soleymani, and L. Boulon. Towards health-aware energy management strategies in fuel cell hybrid electric vehicles: A review. *International Journal of Hydrogen Energy*, 47(17):10021–10043, 2 2022. ISSN 03603199. doi: 10.1016/J.IJHYDENE.2022.01.064.
- [16] Junye Wang, Hualin Wang, and Yi Fan. Techno-economic challenges of fuel cell commercialization. *Engineering*, 4(3):352–360, 2018. ISSN 2095-8099. doi: <https://doi.org/10.1016/j.eng.2018.05.007>. URL <https://www.sciencedirect.com/science/article/pii/S2095809917307750>.
- [17] Ke Song, Xiaodi Wang, Feiqiang Li, Marco Sorrentino, and Bailin Zheng. Pontryagin’s minimum principle-based real-time energy management strategy for fuel cell hybrid electric vehicle considering both fuel economy and power source durability. *Energy*, 205:118064, 2020. ISSN 0360-5442. doi: <https://doi.org/10.1016/j.energy.2020.118064>. URL <https://www.sciencedirect.com/science/article/pii/S0360544220311713>.
- [18] Kaile Zhou and Shanlin Yang. 5.11 smart energy management. In Ibrahim Dincer, editor, *Comprehensive Energy Systems*, pages 423–456. Elsevier, Oxford, 2018. ISBN 978-0-12-814925-6. doi: <https://doi.org/10.1016/B978-0-12-809597-3.00525-3>. URL <https://www.sciencedirect.com/science/article/pii/B9780128095973005253>.
- [19] Di Zhu, Ewan Pritchard, Sumanth Reddy Dadam, Vivek Kumar, and Yang Xu. Optimization of rule-based energy management strategies for hybrid vehicles using dynamic programming. *Combustion Engines*, 184(1):3–10, 7 2022. doi: 10.19206/CE-131967. URL <http://arxiv.org/abs/2207.06450><http://dx.doi.org/10.19206/CE-131967>.
- [20] Xiaosong Hu, Changfu Zou, Xiaolin Tang, Teng Liu, and Lin Hu. Cost-optimal energy management of hybrid electric vehicles using fuel cell/battery health-aware predictive control. *IEEE Transactions on Power Electronics*, 35(1):382–392, 1 2020. ISSN 19410107. doi: 10.1109/TPEL.2019.2915675.
- [21] Xueqin Lü, Yinbo Wu, Jie Lian, Yangyang Zhang, Chao Chen, Peisong Wang, and Lingzheng Meng. Energy management of hybrid electric vehicles: A review of energy optimization of fuel cell hybrid power system based on genetic algorithm. *Energy Conversion and Management*, 205:112474, 2 2020. ISSN 0196-8904. doi: 10.1016/J.ENCONMAN.2020.112474.
- [22] Jian Yang, Tiezhu Zhang, Jichao Hong, Hongxin Zhang, Qinghai Zhao, and Zewen Meng. Research on driving control strategy and Fuzzy logic optimization of a novel mechatronics-electrohydraulic power coupling electric vehicle. *Energy*, 233:121221, 10 2021. ISSN 0360-5442. doi: 10.1016/J.ENERGY.2021.121221.
- [23] Peilin Xie, Sen Tan, Najmeh Bazmohammadi, Josep M. Guerrero, and Juan C. Vasquez. A Real-Time Power Management Strategy for Hybrid Electrical Ships Under Highly Fluctuated Propulsion Loads. *IEEE Systems Journal*, 2022. ISSN 19379234. doi: 10.1109/JSYST.2022.3177843.
- [24] João Pedro Fernandes Trovão and Paulo José Gameiro Pereirinha. Control scheme for hybridised electric vehicles with an online power follower management strategy. *IET Electrical Systems in Transportation*, 5(1):12–23, 3 2015. ISSN 20429746. doi: 10.1049/IET-EST.2013.0038.
- [25] Philipp J. Tritschler, Seddik Bacha, Elisabeth Rullière, and Geoffroy Husson. Energy management strategies for an embedded fuel cell system on agricultural vehicles. *19th International Conference on Electrical Machines, ICEM 2010*, 2010. doi: 10.1109/ICELMACH.2010.5608314.

- [26] Han Liu, • Alexander Gegov, and Mihaela Cocea. Rule-based systems: a granular computing perspective. *Granular Computing*, 1, 2016. doi: 10.1007/s41066-016-0021-6.
- [27] Shuo Zhang, Rui Xiong, and Fengchun Sun. Model predictive control for power management in a plug-in hybrid electric vehicle with a hybrid energy storage system. *Applied Energy*, 185: 1654–1662, 1 2017. ISSN 03062619. doi: 10.1016/J.APENERGY.2015.12.035.
- [28] Yongqiang Wang, Scott J. Moura, Suresh G. Advani, and Ajay K. Prasad. Power management system for a fuel cell/battery hybrid vehicle incorporating fuel cell and battery degradation. *International Journal of Hydrogen Energy*, 44(16):8479–8492, 3 2019. ISSN 0360-3199. doi: 10.1016/J.IJHYDENE.2019.02.003.
- [29] Hongliang Jiang, Liangfei Xu, Jianqiu Li, Zunyan Hu, and Minggao Ouyang. Energy management and component sizing for a fuel cell/battery/supercapacitor hybrid powertrain based on two-dimensional optimization algorithms. *Energy*, 177:386–396, 6 2019. ISSN 0360-5442. doi: 10.1016/J.ENERGY.2019.04.110.
- [30] Ke Song, Xiaodi Wang, Feiqiang Li, Marco Sorrentino, and Bailin Zheng. Pontryagin’s minimum principle-based real-time energy management strategy for fuel cell hybrid electric vehicle considering both fuel economy and power source durability. *Energy*, 205:118064, 8 2020. ISSN 0360-5442. doi: 10.1016/J.ENERGY.2020.118064.
- [31] Fengqi Zhang, Lihua Wang, Serdar Coskun, Hui Pang, Yahui Cui, and Junqiang Xi. Energy management strategies for hybrid electric vehicles: Review, classification, comparison, and outlook. *Energies*, 13(13), 2020. ISSN 1996-1073. doi: 10.3390/en13133352. URL <https://www.mdpi.com/1996-1073/13/13/3352>.
- [32] M. Kalikatzarakis, R. D. Geertsma, E. J. Boonen, K. Visser, and R. R. Negenborn. Ship energy management for hybrid propulsion and power supply with shore charging. *Control Engineering Practice*, 76:133–154, 7 2018. ISSN 09670661. doi: 10.1016/J.CONENGPRAC.2018.04.009.
- [33] Fengqi Zhang, Lihua Wang, Serdar Coskun, Hui Pang, Yahui Cui, and Junqiang Xi. Energy management strategies for hybrid electric vehicles: Review, classification, comparison, and outlook. *Energies*, 13(13), 7 2020. ISSN 19961073. doi: 10.3390/EN13133352.
- [34] Peilin Xie, Sen Tan, Josep M. Guerrero, and Juan C. Vasquez. MPC-informed ECMS based real-time power management strategy for hybrid electric ship. *Energy Reports*, 7:126–133, 4 2021. ISSN 2352-4847. doi: 10.1016/J.EGYR.2021.02.013.
- [35] Lorenzo Serrao, Simona Onori, and Giorgio Rizzoni. A comparative analysis of energy management strategies for hybrid electric vehicles. *Journal of Dynamic Systems, Measurement and Control, Transactions of the ASME*, 133(3), 5 2011. ISSN 00220434. doi: 10.1115/1.4003267/456399. URL <https://asmedigitalcollection.asme.org/dynamicsystems/article/133/3/031012/456399/A-Comparative-Analysis-of-Energy-Management>.
- [36] Chan-Chiao Lin, Huei Peng, and J W Grizzle. A stochastic control strategy for hybrid electric vehicles. In *Proceedings of the 2004 American Control Conference*, volume 5, pages 4710–4715, 2004. doi: 10.23919/ACC.2004.1384056.
- [37] Seongwan Kim and Jongsu Kim. Optimal Energy Control of Battery Hybrid System for Marine Vessels by Applying Neural Network Based on Equivalent Consumption Minimization Strategy. *Journal of Marine Science and Engineering* 2021, Vol. 9, Page 1228, 9(11):1228, 11 2021. ISSN 2077-1312. doi: 10.3390/JMSE9111228. URL <https://www.mdpi.com/2077-1312/9/11/1228/> [htmhttps://www.mdpi.com/2077-1312/9/11/1228](https://www.mdpi.com/2077-1312/9/11/1228).
- [38] Pemmareddy Saiteja and B. Ashok. Critical review on structural architecture, energy control strategies and development process towards optimal energy management in hybrid vehicles. *Renewable and Sustainable Energy Reviews*, 157:112038, 4 2022. ISSN 1364-0321. doi: 10.1016/J.RSER.2021.112038.

- [39] Tom Fletcher, Rob Thring, and Martin Watkinson. An Energy Management Strategy to concurrently optimise fuel consumption & PEM fuel cell lifetime in a hybrid vehicle. *International Journal of Hydrogen Energy*, 41(46):21503–21515, 12 2016. ISSN 03603199. doi: 10.1016/J.IJHYDENE.2016.08.157.
- [40] Yang Zhou, Alexandre Ravey, and Marie Cécile Péra. Real-time cost-minimization power-allocating strategy via model predictive control for fuel cell hybrid electric vehicles. *Energy Conversion and Management*, 229:113721, 2 2021. ISSN 0196-8904. doi: 10.1016/J.ENCONMAN.2020.113721.
- [41] Xiang Meng, Qi Li, Guorui Zhang, Tianhong Wang, Weirong Chen, and Taiqiang Cao. A dual-mode energy management strategy considering fuel cell degradation for energy consumption and fuel cell efficiency comprehensive optimization of hybrid vehicle. *IEEE Access*, 7:134475–134487, 2019. ISSN 21693536. doi: 10.1109/ACCESS.2019.2939047.
- [42] Zehui Zhang, Cong Guan, and Zhiyong Liu. Real-Time Optimization Energy Management Strategy for Fuel Cell Hybrid Ships Considering Power Sources Degradation. *IEEE Access*, 2020. doi: 10.1109/ACCESS.2020.2991519.
- [43] Chiara Dall’armi, Davide Pivetta, and Rodolfo Taccani. Health-Conscious Optimization of Long-Term Operation for Hybrid PEMFC Ship Propulsion Systems. *Energies 2021, Vol. 14, Page 3813*, 14(13):3813, 6 2021. ISSN 1996-1073. doi: 10.3390/EN14133813. URL <https://www.mdpi.com/1996-1073/14/13/3813/htm><https://www.mdpi.com/1996-1073/14/13/3813>.
- [44] Scott J Moura, Jeffrey L Stein, and Hosam K Fathy. Battery-health conscious power management in plug-in hybrid electric vehicles via electrochemical modeling and stochastic control. *IEEE Transactions on Control Systems Technology*, 21(3):679–694, 2012.
- [45] Meiling Yue, Samir Jemei, and Noureddine Zerhouni. Health-conscious energy management for fuel cell hybrid electric vehicles based on prognostics-enabled decision-making. *IEEE Transactions on Vehicular Technology*, 68(12):11483–11491, 2019.
- [46] Wiljan Vermeer, Gautham Ram Chandra Mouli, and Pavol Bauer. A Comprehensive Review on the Characteristics and Modeling of Lithium-Ion Battery Aging. *IEEE Transactions on Transportation Electrification*, 8(2):2205–2232, 6 2022. ISSN 23327782. doi: 10.1109/TTE.2021.3138357.
- [47] H2C Boat | Sailing Innovation Centre — [sailinginnovationcentre.nl](https://www.sailinginnovationcentre.nl/h2c-boat/). <https://www.sailinginnovationcentre.nl/h2c-boat/>. [Accessed 06-Jun-2023].
- [48] Juan Pablo Rivera-Barrera, Nicolás Muñoz-Galeano, and Henry Omar Sarmiento-Maldonado. electronics SoC Estimation for Lithium-ion Batteries: Review and Future Challenges. *Electronics*, 6, 2017. doi: 10.3390/electronics6040102. URL [www.mdpi.com/journal/electronics](http://www.mdpi.com/journal/electronics).
- [49] Yuan Zou, Xiaosong Hu, Hongmin Ma, and Shengbo Eben Li. Combined State of Charge and State of Health estimation over lithium-ion battery cell cycle lifespan for electric vehicles. *Journal of Power Sources*, 273:793–803, 1 2015. ISSN 03787753. doi: 10.1016/J.JPOWSOUR.2014.09.146.
- [50] Ningyuan Guo, Xudong Zhang, Yuan Zou, Lingxiong Guo, and Guodong Du. Real-time predictive energy management of plug-in hybrid electric vehicles for coordination of fuel economy and battery degradation. *Energy*, 214, 1 2021. ISSN 03605442. doi: 10.1016/J.ENERGY.2020.119070.
- [51] Dickson N.T. How, M. A. Hannan, M. S. Hossain Lipu, and Pin Jern Ker. State of Charge Estimation for Lithium-Ion Batteries Using Model-Based and Data-Driven Methods: A Review. *IEEE Access*, 7:136116–136136, 2019. ISSN 21693536. doi: 10.1109/ACCESS.2019.2942213.
- [52] Xiaosong Hu, Shengbo Li, and Huei Peng. A comparative study of equivalent circuit models for Li-ion batteries. *Journal of Power Sources*, 198:359–367, 1 2012. ISSN 03787753. doi: 10.1016/J.JPOWSOUR.2011.10.013.

- [53] Xin Lai, Yuejiu Zheng, and Tao Sun. A comparative study of different equivalent circuit models for estimating state-of-charge of lithium-ion batteries. *Electrochimica Acta*, 259:566–577, 1 2018. ISSN 0013-4686. doi: 10.1016/J.ELECTACTA.2017.10.153.
- [54] Hongwen He, Rui Xiong, and Jinxin Fan. Evaluation of lithium-ion battery equivalent circuit models for state of charge estimation by an experimental approach. *Energies*, 4(4):582–598, 2011. ISSN 19961073. doi: 10.3390/EN4040582.
- [55] Yi Hsien Chiang, Wu Yang Sean, and Jia Cheng Ke. Online estimation of internal resistance and open-circuit voltage of lithium-ion batteries in electric vehicles. *Journal of Power Sources*, 196(8):3921–3932, 4 2011. ISSN 0378-7753. doi: 10.1016/J.JPOWSOUR.2011.01.005.
- [56] Peng Wu, Julius Partridge, and Richard Bucknall. Cost-effective reinforcement learning energy management for plug-in hybrid fuel cell and battery ships. *Applied Energy*, 275:115258, 10 2020. ISSN 0306-2619. doi: 10.1016/J.APENERGY.2020.115258.
- [57] Dima Fares, Riad Chedid, Ferdinand Panik, Sami Karaki, and Rabih Jabr. Dynamic programming technique for optimizing fuel cell hybrid vehicles. *International Journal of Hydrogen Energy*, 40(24):7777–7790, 6 2015. ISSN 0360-3199. doi: 10.1016/J.IJHYDENE.2014.12.120.
- [58] Lijin Han, Ke Yang, Tian Ma, Ning kang Yang, Hui Liu, and Lingxiong Guo. Battery life constrained real-time energy management strategy for hybrid electric vehicles based on reinforcement learning. *Energy*, 259, 11 2022. ISSN 03605442. doi: 10.1016/J.ENERGY.2022.124986.
- [59] Xiaodong Xu, Shengjin Tang, Huahua Ren, Xuebing Han, Yu Wu, Languang Lu, Xuning Feng, Chuanqiang Yu, Jian Xie, Minggao Ouyang, Wei Liu, and Yuejun Yan. Joint state estimation of lithium-ion batteries combining improved equivalent circuit model with electrochemical mechanism and diffusion process. *Journal of Energy Storage*, 56, 12 2022. ISSN 2352152X. doi: 10.1016/J.EST.2022.106135.
- [60] Shradhdha Sarvaiya, Sachin Ganesh, and Bin Xu. Comparative analysis of hybrid vehicle energy management strategies with optimization of fuel economy and battery life. *Energy*, 228:120604, 8 2021. ISSN 0360-5442. doi: 10.1016/J.ENERGY.2021.120604.
- [61] Adel Merabet, Khandker Tawfique Ahmed, Hussein Ibrahim, Rachid Beguenane, and Amer M.Y.M. Ghias. Energy Management and Control System for Laboratory Scale Microgrid Based Wind-PV-Battery. *IEEE Transactions on Sustainable Energy*, 8(1):145–154, 1 2017. ISSN 19493029. doi: 10.1109/TSTE.2016.2587828.
- [62] Jingang Han, Jean Frederic Charpentier, and Tianhao Tang. An Energy Management System of a Fuel Cell/Battery Hybrid Boat. *Energies 2014, Vol. 7, Pages 2799-2820*, 7(5):2799–2820, 4 2014. ISSN 1996-1073. doi: 10.3390/EN7052799. URL <https://www.mdpi.com/1996-1073/7/5/2799/htm><https://www.mdpi.com/1996-1073/7/5/2799>.
- [63] Ameen M. Bassam, Alexander B. Phillips, Stephen R. Turnock, and Philip A. Wilson. Development of a multi-scheme energy management strategy for a hybrid fuel cell driven passenger ship. *International Journal of Hydrogen Energy*, 42(1):623–635, 1 2017. ISSN 03603199. doi: 10.1016/J.IJHYDENE.2016.08.209.
- [64] Flavio Balsamo, Clemente Capasso, Davide Lauria, and Ottorino Veneri. Optimal design and energy management of hybrid storage systems for marine propulsion applications. *Applied Energy*, 278:115629, 11 2020. ISSN 0306-2619. doi: 10.1016/J.APENERGY.2020.115629.
- [65] Lino Guzzella and Antonio Sciarretta. *Vehicle Propulsion Systems : Introduction to Modeling and Optimization*, volume 3. Springer, Berlin, 3 edition, 2015. ISBN 9783540746911.
- [66] M. Safari, M. Morcrette, A. Teysot, and C. Delacourt. Multimodal Physics-Based Aging Model for Life Prediction of Li-Ion Batteries. *Journal of The Electrochemical Society*, 156(3):A145, 12 2009. ISSN 00134651. doi: 10.1149/1.3043429/XML. URL <https://iopscience.iop.org/article/10.1149/1.3043429><https://iopscience.iop.org/article/10.1149/1.3043429/meta>.

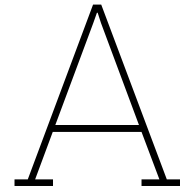
- [67] Anthony Barré, Benjamin Deguilhem, Sébastien Grolleau, Mathias Gérard, Frédéric Suard, and Delphine Riu. A review on lithium-ion battery ageing mechanisms and estimations for automotive applications. *Journal of Power Sources*, 241:680–689, 11 2013. ISSN 0378-7753. doi: 10.1016/J.JPOWSOUR.2013.05.040.
- [68] Matthew B. Pinson and Martin Z. Bazant. Theory of SEI Formation in Rechargeable Batteries: Capacity Fade, Accelerated Aging and Lifetime Prediction. *Journal of The Electrochemical Society*, 160(2):A243–A250, 12 2013. ISSN 0013-4651. doi: 10.1149/2.044302JES/XML. URL <https://iopscience.iop.org/article/10.1149/2.044302jeshttps://iopscience.iop.org/article/10.1149/2.044302jes/meta>.
- [69] Xin Sui, Shan He, Søren B. Vilsen, Jinhao Meng, Remus Teodorescu, and Daniel Ioan Stroe. A review of non-probabilistic machine learning-based state of health estimation techniques for Lithium-ion battery. *Applied Energy*, 300, 10 2021. ISSN 03062619. doi: 10.1016/J.APENERGY.2021.117346.
- [70] Harry J. Ploehn, Premanand Ramadass, and Ralph E. White. Solvent diffusion model for aging of lithium-ion battery cells. *Journal of The Electrochemical Society*, 151, 2004.
- [71] A. J. Smith, J. C. Burns, D. Xiong, and J. R. Dahn. Interpreting high precision coulometry results on li-ion cells. *Journal of The Electrochemical Society*, 158(10):A1136, aug 2011. doi: 10.1149/1.3625232. URL <https://dx.doi.org/10.1149/1.3625232>.
- [72] Ramaraja P. Ramasamy, Jong-Won Lee, and Branko N. Popov. Simulation of capacity loss in carbon electrode for lithium-ion cells during storage. *Journal of Power Sources*, 166(1):266–272, 2007. ISSN 0378-7753. doi: <https://doi.org/10.1016/j.jpowsour.2006.12.086>. URL <https://www.sciencedirect.com/science/article/pii/S0378775307000924>.
- [73] S. Mekhilef, R. Saidur, and A. Safari. Comparative study of different fuel cell technologies. *Renewable and Sustainable Energy Reviews*, 16(1):981–989, 1 2012. ISSN 1364-0321. doi: 10.1016/J.RSER.2011.09.020.
- [74] Lindert van Biert and Klaas Visser. *Chapter 3 - Fuel cells systems for sustainable ships*. Elsevier, 2022. ISBN 978-0-12-824471-5. doi: <https://doi.org/10.1016/B978-0-12-824471-5.00010-4>. URL <https://www.sciencedirect.com/science/article/pii/B9780128244715000104>.
- [75] Ronald F. Mann, John C. Amphlett, Michael A.I. Hooper, Heidi M. Jensen, Brant A. Peppley, and Pierre R. Roberge. Development and application of a generalised steady-state electrochemical model for a PEM fuel cell. *Journal of Power Sources*, 86(1-2):173–180, 3 2000. ISSN 0378-7753. doi: 10.1016/S0378-7753(99)00484-X.
- [76] L. Guzzella and A. Amstutz. Cae tools for quasi-static modeling and optimization of hybrid powertrains. *IEEE Transactions on Vehicular Technology*, 48(6):1762–1769, 1999. doi: 10.1109/25.806768.
- [77] Vishal O Mittal, H Russell Kunz, and James M Fenton. Membrane degradation mechanisms in pemfcs. *Journal of The Electrochemical Society*, 154(7):B652, 2007.
- [78] Marine Jouin, Rafael Gouriveau, Daniel Hissel, Marie Cécile Péra, and Noureddine Zerhouni. Degradations analysis and aging modeling for health assessment and prognostics of PEMFC. *Reliability Engineering & System Safety*, 148:78–95, 4 2016. ISSN 0951-8320. doi: 10.1016/J.RESS.2015.12.003.
- [79] F. A. De Bruijn, V. A.T. Dam, and G. J.M. Janssen. Review: Durability and degradation issues of PEM fuel cell components. *Fuel Cells*, 8(1):3–22, 2 2008. ISSN 16156846. doi: 10.1002/FUCE.200700053.
- [80] Jinfeng Wu, Xiao Zi Yuan, Jonathan J. Martin, Haijiang Wang, Jiujun Zhang, Jun Shen, Shaohong Wu, and Walter Merida. A review of PEM fuel cell durability: Degradation mechanisms and mitigation strategies. *Journal of Power Sources*, 184(1):104–119, 9 2008. ISSN 0378-7753. doi: 10.1016/J.JPOWSOUR.2008.06.006.

- [81] Junjie Zhao, Zhengkai Tu, and Siew Hwa Chan. Carbon corrosion mechanism and mitigation strategies in a proton exchange membrane fuel cell (PEMFC): A review. *Journal of Power Sources*, 488:229434, 3 2021. ISSN 0378-7753. doi: 10.1016/J.JPOWSOUR.2020.229434.
- [82] Huicui Chen, Pucheng Pei, and Mancun Song. Lifetime prediction and the economic lifetime of Proton Exchange Membrane fuel cells. *Applied Energy*, 142:154–163, 3 2015. ISSN 0306-2619. doi: 10.1016/J.APENERGY.2014.12.062.
- [83] Pucheng Pei, Qianfei Chang, and Tian Tang. A quick evaluating method for automotive fuel cell lifetime. *International Journal of Hydrogen Energy*, 33(14):3829–3836, 2008. ISSN 0360-3199. doi: <https://doi.org/10.1016/j.ijhydene.2008.04.048>. URL <https://www.sciencedirect.com/science/article/pii/S036031990800476X>. TMS07: Symposium on Materials in Clean Power Systems.
- [84] Y.Y. Mamrybayeva, R.E. Beissenov, Mkhitar Hobosyan, S.E. Kumekov, and Karen Martirosyan. Charge and discharge behaviour of li-ion batteries at various temperatures containing licoo2 nanostructured cathode produced by ccso. *Eurasian Chemico-Technological Journal*, 15:301, 11 2015. doi: 10.18321/ectj235.
- [85] Ke Song, Yuhang Ding, Xiao Hu, Hongjie Xu, Yimin Wang, and Jing Cao. Degradation adaptive energy management strategy using fuel cell state-of-health for fuel economy improvement of hybrid electric vehicle. *Applied Energy*, 285, 3 2021. ISSN 03062619. doi: 10.1016/J.APENERGY.2020.116413.
- [86] D. Pivetta, C. Dall’Armi, and R. Tacconi. Multi-objective optimization of hybrid PEMFC/Li-ion battery propulsion systems for small and medium size ferries. *International Journal of Hydrogen Energy*, 46(72):35949–35960, 10 2021. ISSN 0360-3199. doi: 10.1016/J.IJHYDENE.2021.02.124.
- [87] Bolun Xu, Alexandre Oudalov, Andreas Ulbig, Göran Andersson, and Daniel S Kirschen. Modeling of lithium-ion battery degradation for cell life assessment. *IEEE Transactions on Smart Grid*, 9(2):1131–1140, 2016.
- [88] Daniel Ioan Stroe. Lifetime models for lithium-ion batteries used in virtual power plant applications. 2014.
- [89] Hector Eduardo Perez, Xiaosong Hu, Satadru Dey, and Scott J. Moura. Optimal charging of li-ion batteries with coupled electro-thermal-aging dynamics. *IEEE Transactions on Vehicular Technology*, 66(9):7761–7770, 2017. doi: 10.1109/TVT.2017.2676044.
- [90] Felix Grasser and Alfred C Rufer. A fully analytical pem fuel cell system model for control applications. In *Conference Record of the 2006 IEEE Industry Applications Conference Forty-First IAS Annual Meeting*, volume 5, pages 2162–2168. IEEE, 2006.
- [91] Fabio Musio, Fausto Tacchi, Luca Omati, Paola Gallo Stampino, Giovanni Dotelli, Stefano Limonta, Davide Brivio, and Paolo Grassini. Pemfc system simulation in matlab-simulink® environment. *International Journal of Hydrogen Energy*, 36(13):8045–8052, 2011.
- [92] N Ouddah, Moussa Boukhnifer, and A Raisemche. Two control energy management schemes for electrical hybrid vehicle. In *10th international multi-conferences on systems, signals & devices 2013 (SSD13)*, pages 1–6. IEEE, 2013.
- [93] Mehdi Ansarey, Masoud Shariat Panahi, Hussein Ziarati, and Mohammad Mahjoob. Optimal energy management in a dual-storage fuel-cell hybrid vehicle using multi-dimensional dynamic programming. *Journal of Power Sources*, 250:359–371, 2014.
- [94] Shirin Espiari and Majid Aleyaasin. Transient response of pem fuel cells during sudden load change. In *2010 IEEE International Energy Conference*, pages 211–216, 2010. doi: 10.1109/ENERGYCON.2010.5771678.

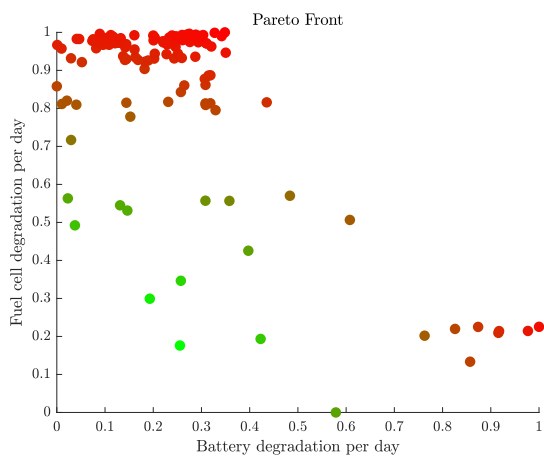
- [95] Jacqueline S. Edge, Simon O'Kane, Ryan Prosser, Niall D. Kirkaldy, Anisha N. Patel, Alastair Hales, Abir Ghosh, Weilong Ai, Jingyi Chen, Jiang Yang, and et al. Lithium ion battery degradation: What you need to know. *Physical Chemistry Chemical Physics*, 23(14):8200–8221, 2021. doi: 10.1039/d1cp00359c.
- [96] Anthony Barré, Benjamin Deguilhem, Sébastien Grolleau, Mathias Gérard, Frédéric Suard, and Delphine Riu. A review on lithium-ion battery ageing mechanisms and estimations for automotive applications. *Journal of Power Sources*, 241:680–689, 2013. ISSN 0378-7753. doi: <https://doi.org/10.1016/j.jpowsour.2013.05.040>. URL <https://www.sciencedirect.com/science/article/pii/S0378775313008185>.
- [97] Xuebing Han, Languang Lu, Yuejiu Zheng, Xuning Feng, Zhe Li, Jianqiu Li, and Minggao Ouyang. A review on the key issues of the lithium ion battery degradation among the whole life cycle. *eTransportation*, 1:100005, 2019. ISSN 2590-1168. doi: <https://doi.org/10.1016/j.etrans.2019.100005>. URL <https://www.sciencedirect.com/science/article/pii/S2590116819300050>.
- [98] Seong Jin An, Jianlin Li, Claus Daniel, Debasish Mohanty, Shrikant Nagpure, and David L. Wood. The state of understanding of the lithium-ion-battery graphite solid electrolyte interphase (sei) and its relationship to formation cycling. *Carbon*, 105:52–76, 2016. ISSN 0008-6223. doi: <https://doi.org/10.1016/j.carbon.2016.04.008>. URL <https://www.sciencedirect.com/science/article/pii/S0008622316302676>.
- [99] Jacqueline S. Edge, Simon O'Kane, Ryan Prosser, Niall D. Kirkaldy, Anisha N. Patel, Alastair Hales, Abir Ghosh, Weilong Ai, Jingyi Chen, Jiang Yang, Shen Li, Mei Chin Pang, Laura Bravo Diaz, Anna Tomaszewska, M. Waseem Marzook, Karthik N. Radhakrishnan, Huizhi Wang, Yatish Patel, Billy Wu, and Gregory J. Offer. Lithium ion battery degradation: what you need to know. *Physical Chemistry Chemical Physics*, 23(14):8200–8221, 4 2021. ISSN 1463-9084. doi: 10.1039/D1CP00359C. URL <https://pubs.rsc.org/en/content/articlehtml/2021/cp/d1cp00359c><https://pubs.rsc.org/en/content/articlelanding/2021/cp/d1cp00359c>.
- [100] Evelina Wikner and Torbjörn Thiringer. Extending battery lifetime by avoiding high soc. *Applied Sciences*, 8(10), 2018. ISSN 2076-3417. doi: 10.3390/app8101825. URL <https://www.mdpi.com/2076-3417/8/10/1825>.
- [101] Xiaosong Hu, Changfu Zou, Xiaolin Tang, Teng Liu, and Lin Hu. Cost-optimal energy management of hybrid electric vehicles using fuel cell/battery health-aware predictive control. *IEEE Transactions on Power Electronics*, 35(1):382–392, 1 2020. ISSN 19410107. doi: 10.1109/TPEL.2019.2915675.
- [102] Huan Li, Yang Zhou, Hamid Gualous, Hicham Chaoui, and Loic Boulon. Optimal Cost Minimization Strategy for Fuel Cell Hybrid Electric Vehicles Based on Decision-Making Framework. *IEEE Transactions on Industrial Informatics*, 17(4):2388–2399, 4 2021. ISSN 19410050. doi: 10.1109/TII.2020.3003554.
- [103] Yonggang Liu, Junjun Liu, Yuanjian Zhang, Yitao Wu, Zheng Chen, and Ming Ye. Rule learning based energy management strategy of fuel cell hybrid vehicles considering multi-objective optimization. *Energy*, 207:118212, 9 2020. ISSN 0360-5442. doi: 10.1016/J.ENERGY.2020.118212.
- [104] Richard Bellman. Dynamic programming. *Science*, 153(3731):34–37, 1966. ISSN 00368075. doi: 10.1126/SCIENCE.153.3731.34.
- [105] Olle Sundstrom and Lino Guzzella. A generic dynamic programming matlab function. In *2009 IEEE control applications,(CCA) & intelligent control,(ISIC)*, pages 1625–1630. IEEE, 2009.
- [106] R. Bellman, Rand Corporation, and Karreman Mathematics Research Collection. *Dynamic Programming*. Rand Corporation research study. Princeton University Press, 1957. ISBN 9780691079516. URL <https://books.google.nl/books?id=wdtoPwAACAAJ>.
- [107] Xiaobin Li, Yuxin Zhang, Yi Peng, Wenqing Zhang, Shiyue Zhang, and Xuefang Li. Reinforcement learning-based energy management for plug-in hybrid electric vehicles. In *2023 9th International Conference on Electrical Engineering, Control and Robotics (EECR)*, pages 1–6, 2023. doi: 10.1109/EECR56827.2023.10150124.

- [108] Nan Zhao, Fengqi Zhang, Yalian Yang, Serdar Coskun, Xianke Lin, and Xiaosong Hu. Dynamic traffic prediction-based energy management of connected plug-in hybrid electric vehicles with long short-term state of charge planning. *IEEE Transactions on Vehicular Technology*, 72(5): 5833–5846, 2023. doi: 10.1109/TVT.2022.3229700.
- [109] Stefano Leonori, Cristina Moscatiello, Maria Carmen Falvo, and Fabio Massimo Frattale Mascioli. Smart integration and energy optimization of evs charging systems in a nanogrid. In *2023 IEEE International Conference on Electrical Systems for Aircraft, Railway, Ship Propulsion and Road Vehicles & International Transportation Electrification Conference (ESARS-ITEC)*, pages 1–6, 2023. doi: 10.1109/ESARS-ITEC57127.2023.10114889.
- [110] Zhiyan Feng, Fei Jiang, Miao Cao, Bizhou Mei, and Shengdun Zhao. Multi-objective optimization and performance comparison of different driving configurations of in-wheel motors. *IEEE Access*, 11:53144–53154, 2023. doi: 10.1109/ACCESS.2023.3278258.
- [111] Bastian Krueger, Giovanni Filomeno, Arnd Golle, Dirk Dennin, and Peter Tenberge. Unified mode-based description of arbitrary hybrid and electric powertrain topologies. *IEEE Transactions on Vehicular Technology*, 71(2):1293–1306, 2022. doi: 10.1109/TVT.2021.3133790.
- [112] Atriya Biswas, Pier Giuseppe Anselma, and Ali Emadi. Real-time optimal energy management of multimode hybrid electric powertrain with online trainable asynchronous advantage actor–critic algorithm. *IEEE Transactions on Transportation Electrification*, 8(2):2676–2694, 2022. doi: 10.1109/TTE.2021.3138330.
- [113] Pedro M. Muñoz, Gabriel Correa, Marcos E. Gaudiano, and Damián Fernández. Energy management control design for fuel cell hybrid electric vehicles using neural networks. *International Journal of Hydrogen Energy*, 42(48):28932–28944, 11 2017. ISSN 0360-3199. doi: 10.1016/J.IJHYDENE.2017.09.169.
- [114] Zhenyu Huang, Jun Shen, Siew Hwa Chan, and Zhengkai Tu. Transient response of performance in a proton exchange membrane fuel cell under dynamic loading. *Energy Conversion and Management*, 226:113492, 2020. ISSN 0196-8904. doi: <https://doi.org/10.1016/j.enconman.2020.113492>. URL <https://www.sciencedirect.com/science/article/pii/S0196890420310244>.
- [115] Yuanli Ding, Zachary P Cano, Aiping Yu, Jun Lu, and Zhongwei Chen. Automotive li-ion batteries: current status and future perspectives. *Electrochemical Energy Reviews*, 2:1–28, 2019.
- [116] David Feldman, Vignesh Ramasamy, Ran Fu, Ashwin Ramdas, Jal Desai, and Robert Margolis. Us solar photovoltaic system and energy storage cost benchmark (q1 2020). Technical report, National Renewable Energy Lab.(NREL), Golden, CO (United States), 2021.
- [117] Wesley Cole, A Will Frazier, and Chad Augustine. Cost projections for utility-scale battery storage: 2021 update. Technical report, National Renewable Energy Lab.(NREL), Golden, CO (United States), 2021.
- [118] Meiling Yue, Zeina Al Masry, Samir Jemei, and Nouredine Zerhouni. An online prognostics-based health management strategy for fuel cell hybrid electric vehicles. *International Journal of Hydrogen Energy*, 46(24):13206–13218, 4 2021. ISSN 0360-3199. doi: 10.1016/J.IJHYDENE.2021.01.095.
- [119] Hui Chen, Zehui Zhang, Cong Guan, and Haibo Gao. Optimization of sizing and frequency control in battery/supercapacitor hybrid energy storage system for fuel cell ship. *Energy*, 197: 117285, 4 2020. ISSN 0360-5442. doi: 10.1016/J.ENERGY.2020.117285.
- [120] Kyaw Hein. Emission-aware and data-driven many-objective voyage and energy management optimization of solar-integrated all-electric ship. *Electric Power Systems Research*, 213, 12 2022. ISSN 03787796. doi: 10.1016/J.EPSR.2022.108718.

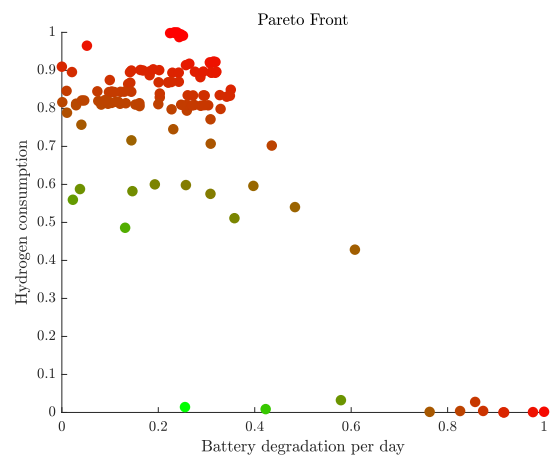




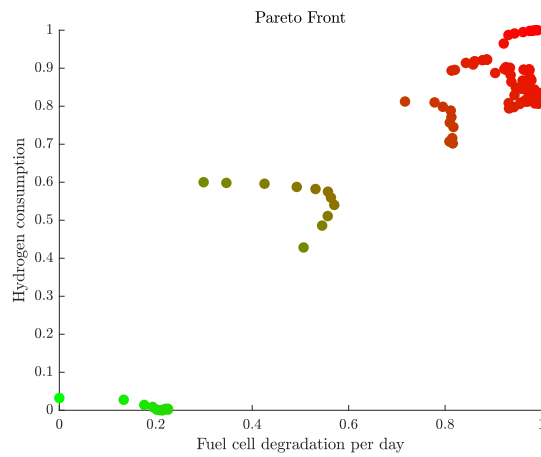
# Pareto-fronts



(a) Pareto-front between fuel cell degradation and battery degradation



(b) Pareto-front between hydrogen consumption and battery degradation



(c) Pareto-front hydrogen consumption and fuel cell degradation

Figure A.1: Three different perspectives of the Pareto-front





## B

## Health aware Energy Management Systems literature

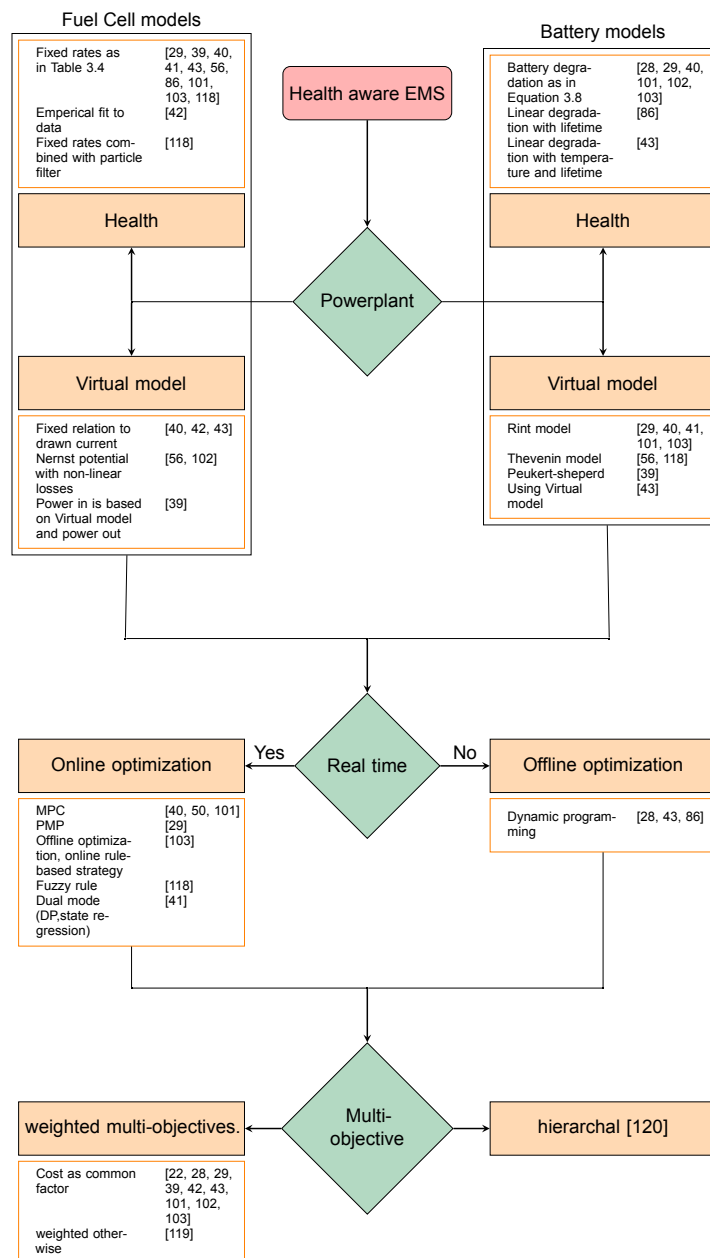


Figure B.1: Health aware EMS's